Advances in integration of photovoltaic power and energy production in practical systems

Tomás Oliveira Fartaria

Tese apresentada à Universidade de Évora
para obtenção do Grau de Doutor em Engenharia Mecatrónica e Energia
Especialidade: Energia

ORIENTADOR: *Professor Doutor Manuel Collares-Pereira*

ÉVORA, Agosto 2016

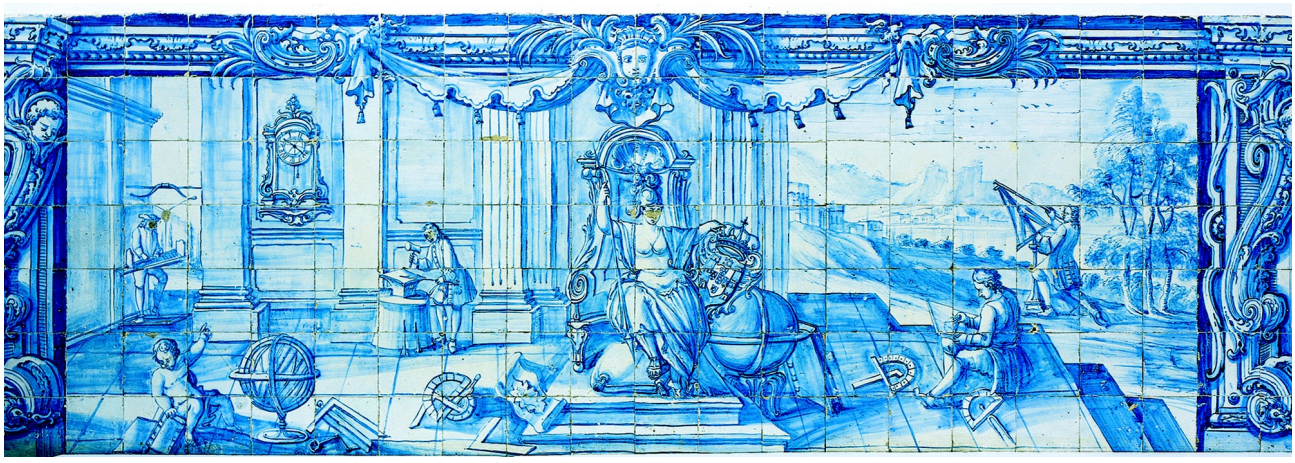

INSTITUTO DE INVESTIGAÇÃO E FORMAÇÃO AVANÇADA

UNIVERSIDADE DE ÉVORA

Instituto de Investigação e Formação Avançada

Departamento de Física

Advances in integration of photovoltaic power and energy production in practical systems

Tomás Oliveira Fartaria

Orientação *Professor Doutor Manuel Pedro Ivens Collares Pereira*

Engenharia Mecatrónica e Energia

Dissertação

1 de Agosto de 2016

Acknowledgements

Despite the name of the author in the thesis front page, this work could never be done without the precious help of many people, either by directly helping to build the demonstrators or by lending a hear, but always rooting for me.

I am eternally grateful to my supervisor Prof. Dr. Manuel Collares Pereira for all the inspiration, guidance, patience, criticism, and everything in between. I will always cherish the many hours spent in trips, discussions, picnics and even card games. Your optimism, ambition and wisdom are an inspiration and model to me.

Secondly, I have to thank my "war" buddies of the Renewable Chair's: Afonso Cavaco, Diogo Canavarro, Hugo Silva, João Marchã, Luís Fialho, Tiago Osório, Ricardo Conceição and many others, aka the "Egyptian Brigade": for the many many days of companionship provided in "the attics" , between many laughs and joys. Thanks for being available for whatever job was needed to be done or for having a drink in the end of the day. It was a pleasure to work by their side and I will always remember the fantastic group spirit, the most important element that made these years so fruitful and enjoyable.

For all the Universities' personnel that have helped me correct my mistakes and deal with the necessary bureaucracy from the beginning until the very end. A special thanks to Assunção Mexia, Ana Prates, Ana Rita, Célia Toureiro, and Carolina Camarinhas for always being helpful and greeting me with a smile.

I also have to acknowledge the support of the Portuguese National Science and Technology Foundation - FCT (Fundação para a Ciência e Tecnologia) - for giving me a PhD scholarship No. SFRH/BD/84396/2012.

To my family (both Fartaria's and Ferreira's) and friends (special thanks to my sister Tânia, friends Cebola, Maria, Tânia Carreira, Armando and Roy) sorry for having to hear me complain throughout this years but without it, I don't believe I would have lasted this long. You helped me put things in perspective and gave me strength and lifted my spirits when I most needed it.

Last but not least, thank you Tânia, my companion and soul mate, for giving me the best years of my life and for making it better and meaningful. You are an infinite source of strength and inspiration.

The very last thanks are to my best furry friend Simba, for being so happy, loyal and present. I am privileged to count you as part of my family.

Contents

Abstract

This thesis presents advances in integration of photovoltaic (PV) power and energy in practical systems, such as existing power plants in buildings or directly integrated in the public electrical grid. It starts by providing an analyze of the current state of PV power and some of its limitations. The work done in this thesis begins by providing a model to compute mutual shading in large PV plants, and after provides a study of the integration of a PV plant in a biogas power plant. The remainder sections focus on the work done for project PVCROPS, which consisted on the construction and operation of two prototypes composed of a PV system and a novel battery connected to a building and to the public electrical grid. These prototypes were then used to test energy management strategies and validate the suitability of the two advanced batteries (a lithium-ion battery and a vanadium redox flow battery) for households (BIPV) and PV plants. This thesis is divided in 7 chapters: Chapter 1 provides an introduction to explain and develop the main research questions studied for this thesis; Chapter 2 presents the development of a ray-tracing model to compute shading in large PV fields (with or without trackers); Chapter 3 shows the simulation of hybridizing a biogas plant with a PV plant, using biogas as energy storage; Chapters 4 and 5 present the construction, programming, and initial operation of both prototypes (Chapter 4), EMS testing oriented to BIPV systems (Chapter 5). Finally, Chapters 6 provides some future lines of investigation that can follow this thesis, and Chapter 7 shows a synopsis of the main conclusions of this work.

Keywords: Photovoltaics and grid interface, Vanadium Redox Flow Battery, Energy Management Strategies

Resumo

Avanços na integração de potência fotovoltaica e produção de energia em sistemas práticos

Esta tese apresenta avanços na integração de potência e energia fotovoltaica (PV) em sistemas práticos, tais como centrais existentes ou a rede eléctrica pública. Começa por analisar o estado corrente do fotovoltaico no mundo e aborda algumas das suas limitações. O trabalho feito para esta tese de doutoramento começou pelo desenvolvimento de um modelo para calcular os sombreamentos que ocorrem em grandes campos fotovoltaicos, e depois apresenta um estudo sobre a integração um sistema fotovoltaico em uma central eléctrica a biogás. As últimas secções da tese focam-se no trabalho feito para o projecto PVCROPS, que consistiu na construção e operação de dois demonstratores, cada um formado por um sistema fotovoltaico e bateria conectados a um edifício e à rede eléctrica pública. Estes protótipos foram posteriormente utilizados para testar estratégias de gestão de energia (EMS) e para validar a operação de duas baterias avançadas (bateria de Iões de Lítio e bateria de Fluxo Redox de Vanádio) e a sua utilização para habitações e centrais PV. A tese está dividida em 7 capítulos: O capítlo 1 apresenta uma introdução para explicar e desenvolver as principais questões que foram investigadas nesta tese; O capítulo 2 mostra o desenvolvimento de um modelo baseado em traçados de raios para calcular sombreamentos mútuos em grandes centrais PV (com e sem seguidores); O capítulo 3 mostra a simulação da hibridização de uma central eléctrica a biogás com uma central PV, e utilizando o biogás como armazenamento de energia. Os capítulos 4 e 5 apresentam a construção, programação e operação inicial dos dois demonstradores (Capítulo 4), o teste de EMS orientadas para sistemas PV em habitações (Capítulo 5). Finalmente, o Capítulo 6 sugere algumas futuras linhas de investigação que poderão seguir esta tese, e o Capítulo 7 faz uma sinopse das principais conclusões deste trabalho.

Palavras-chave: Interface entre Sistemas Fotovoltaicos e rede, Bateria de Fluxo Redox de Vanádio, Gestão de Energia

List of Papers

This thesis includes the following papers:

I. Fartaria, T., Collares Pereira, M., *Simulation and computation of shadow losses of direct normal, diffuse solar radiation and albedo in a photovoltaic field with multiple 2-axis trackers using ray tracing methods*, Solar Energy 91 (2013), pp. 93-101. [Chapter 2]

II. González-González, A., Collares Pereira, M., Cuadros, F., Fartaria, T., *Energy self-sufficiency through hybridization of biogas and photovoltaic solar energy. An application for an Iberian pig slaughterhouse*, Journal of Cleaner Production 65 (2014), pp. 318-323. [Chapter 3]

III. Fialho, L., Fartaria, T., Narvarte, L., Collares Pereira, M., *Implementation and validation of a Self-Consumption Maximization energy management strategy in a Vanadium Redox Flow BIPV demonstrator*, Energies 2016, 9(7), 496, [Chapter 5]

Other presentations and publications related with the subject of the present thesis are:

I. Fialho, L., Fartaria, T., "Demonstrators of Li-ion and Vanadium Redox Batteries", Oral Presentation, European Photovoltaic Solar Energy Conference and Exhibition (2015), Parallel event: "PV CROPS: Novel solutions for a high PV penetration in EU electrical networks with lower LCOE."

II. Fialho, L., Fartaria, T., Collares Pereira, M., *Performance Characterization of a Vanadium Redox Flow Battery*, Poster presentation, European Photovoltaic Solar Energy Conference and Exhibition (2015) Hamburg, Germany

III. Fialho, L., Fartaria, T., Collares Pereira, M., *Validation of a Energy Management Strategy for a BIPV System with a Vanadium Battery Demonstrator*, Poster presentation, European Photovoltaic Solar Energy Conference and Exhibition (2015) Hamburg, Germany

IV. Fialho, L., Fartaria, T., Collares Pereira, M., *Validation of a Energy Management Strategy for a BIPV System with a Lithium Ion Battery Demonstrator*,

Poster presentation, European Photovoltaic Solar Energy Conference and Exhibition (2015) Hamburg, Germany

V. Martinez Moreno, F., Helleputte, F., Tyutyundzhiev, N., Rabal Echeverria, D., Conlon, M., Fartaria, T., Oteiza, D., *Good and bad practices in pv plants.*,European Photovoltaic Solar Energy Conference and Exhibition (2013) Paris, France, pp. 1-3.

List of Figures

List of Tables

Nomenclature

Chapter 1

$BIPV$	Building Integrated PhotoVoltaic
CSP	Concentrated Solar Power
DSO	Distribution System Operator
EMS	Energy Management Strategy
PV	PhotoVoltaic(s)
$PVCROPS$	PhotoVoltaic Cost r€duction, Reliability, Operational performance, Prediction and Simulation
TSO	Transmission System Operator
$UEVORA$	University of Évora
WHO	World Health Organization

Chapter 2

C	Concentration
CPV	Concentrated PhotoVoltaics
$d.n.i.$	Direct Normal Irradiance
PV	PhotoVoltaic(s)
STE	Solar Thermal Electricity
F_{GS}	Geometrical Shadow Factor
N_{SB}	Number of shaded blocks
N_t	Number of time intervals used in the simulations
trk	Tracker

Chapter 3

AD	Anaerobic Digestion
COD	Chemical Oxygen Demand
H_0	Extraterrestrial solar irradiation

H_{col}	Solar irradiation incident on the photovoltaic module
H_d	Diffuse solar irradiation on the Earth's surface
H_h	Monthly average global irradiation on a horizontal surface
HRT	Hydraulic Residence Time
IRR	Internal Rate of Return
NPV	Net Present Value
PBP	PayBack Period
VDS	Volatile Dissolved Solids
VFA	Volatile Fatty Acids
VSS	Volatile Solids in Suspension

Chapter 4

AC	Alternate Current
$BIPV$	Building Integrated PhotoVoltaic
CPU	Central Processing Unit
DC	Direct Current
DOD	Depth of Discharge
EMS	Energy Management Strategy
ESS	Energy Storage System
$FP7$	The Seventh Framework Programme
I_{DC}	Measured DC Current
LIB	Lithium Ion Battery
$MPPT$	Maximum Power Point Tracker
PC	Personal Computer
$PECS$	Plataforma de Ensaio de Colectores Solares (Solar collectors testing platform)
PLC	Programmable Logic Controller
$PVCROPS$	PhotoVoltaic Cost r€duction, Reliability, Operational performance, Prediction and Simulation
$P_{DC\,charge/discharge}$	Measured DC Power during charge/discharge
PV	PhotoVoltaic(s)
RTU	Remote Terminal Unit
SOC	State Of Charge
TCP/IP	Transmission Control Protocol / Internet Protocol

$UEVORA$	University of Évora
$UPNA$	Public University of Navarra
UPS	Uninterruptible Power Supply/Source
$VISA$	Virtual Instrument Software Architecture
$VRFB$	Vanadium Redox Flow Battery
V_{DC}	Measured DC Voltage
η_{ESS}	AC-DC-AC Round-trip Energy Storage System (VRFB + inverters) efficiency
$\eta_{invAC-DC/DC-AC}$	AC to DC/DC to AC inverter conversion efficiency
η_{VRFB}	DC-DC Round-trip VRFB efficiency

Chapter 5

AC	Alternate Current
$BIPV$	Building Integrated PhotoVoltaic
DC	Direct Current
EMS	Energy Management Strategy
ESS	Energy Storage System
FIT	Feed-In-Tariff
$FP7$	The Seventh Framework Programme
$MPPT$	Maximum Power Point Tracker
PC	Personal Computer
PV	PhotoVoltaic(s)
$PVCROPS$	PhotoVoltaic Cost r€duction, Reliability, Operational performance, Prediction and Simulation
SOC	State Of Charge
TCP	Transmission Control Protocol
$VRFB$	Vanadium Redox Flow Battery
P_{bat}	Power to/from the battery
P_{grid}	Power exchanged with the grid measured by the grid wattmeter
$\overline{P_{grid\,15min}}$	15min Averaged Power Grid
P_{inv_bat}	Battery Power measured at the inverter (in the AC side) by the inverter wattmeter
P_{load}	Power consumed by loads
P_{pv}	Power produced by PV system
$P_{residual}$	Residual power

SCR	Self Consumption Ratio

Chapter 1

Introduction

1.1 Background and general motivation

Energy has been one major concern for humanity for centuries. Either for economical, climate, productivity, or health reasons, the production, stoage, and use of energy have always been a vital question. During the last century, non-renewable energies (such as coal, oil, and natural gas) have been the predominant sources of energy on a World scale. The high energy density, stability, and high availability have made these sources of energy highly desirable and easy to use. However, the constant usage of fossil fuels did not come without problems. The burning of oil and coal releases pollutant gases (CO_2, CO, NO_x, SO_x, among other particles) to the atmosphere which is correlated with several climate and health problems, both at a local and global level. According to the World Health Organization (WHO), air pollution is estimated to be responsible for the death of about 7 million people per year (one in eight deaths) and more than half of those deaths are caused by fumes from indoor stoves (still widely used in Africa and Asia) and 90% of the total deaths are from developing countries [2]. Adding to this all the related problems with increasing temperatures that are melting ice caps in the poles, raising sea levels that are forcing entire villages to move, and the several environmental disasters that occurred due to oil spills, among many others. Even a traditionally oil-based industry, automotive, is now rapidly changing to hybrid and all-electric cars. This remarkable change together with the current public perception regarding conventional energy sources, is pushing renewable energies and energy storage technologies to replace the older solutions[1, 3].

The natural solution to solve most of the energy related problems is to use renewable and already distributed sources of energy. With different weights, either sun, wind, waves, or geothermal energy are available in most regions of the globe. These energy sources are clean (don't emit greenhouse gases or other harmful substances) and with major developments made in these areas, renewable electricity can

be cheaper than electricity produced by conventional sources. In the particular case of solar power, Photovoltaics (PV) has been the major booster for its use. PV power can be converted in small modules that can be interconnected to form large plants (centralized or decentralized production), is predictable (along a year despite the hourly/daily variations) and requires minimal maintenance. PV conversion efficiencies in commercial applications range from around 11% for organic, dye-sensitized and Perovskite cells up to 25% for silicon-based technologies (for more details about the major PV technologies and their efficiencies evolution, see Figure 1.1). Considering Concentrated Photovoltaics (cells that use lenses and/or mirrors to focus sunlight in a smaller area), PV cells have reached the staggering 46% world record efficiency, using multi-junction solar cells. Also, the current price of PV panels (at the time of writing, PV prices are close to 70 cents of Euro per Wp) and the long lifetime that they can operate, make this technology perfect to make the transition to clean power generation, even in places with relatively low levels of solar radiation (as is happening in Germany) [4]. With a total installed PV power ascending to

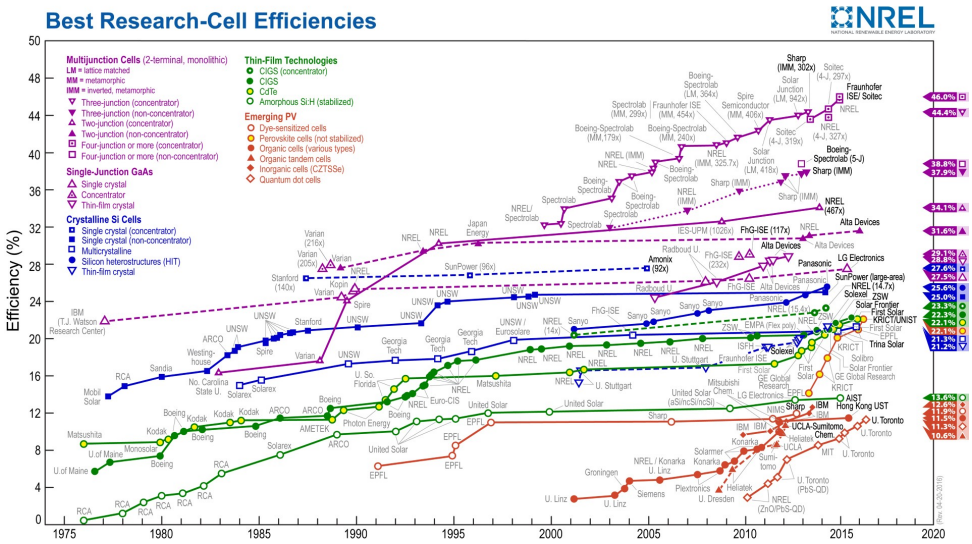

Figure 1.1: Evolution of PV efficiency by technology type.

more than 178 GWp, and mostly concentrated in few countries (Germany, USA, etc.), PV power has become one of the fastest growing and primary choices for new power plants. In fact, PV power has grown so much that some problems that used to be negligible, are nowadays affecting the grid operation and electrical power quality [5]. The most noticeable drawback of PV power is the variation with weather conditions, especially during partially cloudy days. During a year and even a day, solar radiation is highly predictable with the known and expected seasonal and daily variations that occur due to pure geometry (apparent movement of the Sun in the sky). The slow seasonal variation and daily cycle are constant so grid operators,

Transmission System Operators (TSO) and Distribution System Operators (DSO), know that produced PV power will vary accordingly so they can adapt and prepare other power sources and respective power generators to that effect. The only fluctuations that are more difficult to forecast and counteract are short-term fluctuations related to the passage of clouds over PV panels. At a local level (grid level in which PV panels are connected) these variations can be noticeable and might fail grid regulations required of PV plants, but this only happens when a single (or small) PV plant is analyzed. A given cloud only affects a small region at a time and depending on the size and geometry of the PV plant, it can take several seconds/minutes to cover the entire plant. By connecting multiple PV plants, ideally far from each others, those local fluctuations that occur in each PV plant are averaged, reducing their variability to more acceptable levels [6].

PV technology as it is (not considering future improvements in efficiency), is mostly limited to the issue of storing the electricity that is being produced at the moment, to be later used when needed or more necessary. Adding an efficient and affordable energy storage system to a PV plant could solve two problems: attenuate fluctuations hence avoiding the injection of low-quality power into the grid, and store electricity to times when there is no sun or simply to periods when the energy produced is more necessary.

There are many energy storage technologies that function by converting electric energy to some other form, for example: kinetic energy in flywheels, electrochemical energy in batteries, thermal energy in molten salts tanks, gravitational energy in damns, etc. With a storage system connected to the renewable plant, it can absorb production peaks and release that energy later when the production lowers for some reason (clouds or sudden increase of consumption). Very large plants have been using chemical batteries to absorb fluctuations as they must comply with regulations although those batteries have a considerable cost that diminishes the profitability of the plant. Several improvements have been made, especially regarding lithium batteries and the appearance of commercial models of flow batteries, and prices have been falling with the increased demand for cell phones and the new but rapidly increasing market of electric car manufacturers, making batteries more and more economically viable [3, 7, 8].

Another way to approach the power fluctuations problem is to make hybrid generation plants, by combining two or more different renewable energy generators to average the output or explore other more efficient and/or cheaper storage technologies. As said before, even by joining spatially distant PV plants (or wind farms for example), the aggregated power output is less affected by short solar radiation variations and less correlated with local power fluctuations. Some widely used com-

binations of two different renewable generators are wind farms connected to hydro dams with reversible pumps that can store energy by pumping water back into the dam, or molten salts with Concentrated Solar Power (CSP) plants [9].

Several improvements and advances have been made to facilitate the wider penetration of PV (and other renewable energies) in the electrical grid, but certain conditions have only recently appeared: the advent of smart grids, i.e., interconnected equipment (generation and consumption) with monitoring, smart houses, the figure of the "prosumer" (produced and consumer), cheap PV panels, increasing number of electric cars that can act as mobile batteries to be used when they are parked. These, among many other favorable factors, make this moment an excellent time to take developments even further [10].

1.1.1 Research questions

The work described in this thesis aimed to respond to several questions that guided the research process. In the beginning of the Ph.D. program, the following questions arose with no clear answer already provided by previously published research:

- How to model/predict the effect of mutual shading between PV trackers with their modules in large PV plants with multiple configurations and geometries?
- How to improve the integration of PV power in the public grid, i.e., how to combine PV power with other sources to obtain a more stable power output?
- Can batteries perform as expected when used in conjunction with EMS developed to manage PV plants with new batteries connected to the electrical public grid? Do simulations made to test behaviour and generation properly match the real functioning of the new batteries?

1.1.2 The first steps of the PhD thesis

The Ph.D. work began by addressing the first research question which tackles the issue of mutual shading (shadows cast by PV modules on other neighboring PV modules) of PV modules (with or without tracking) in a given field. This is tightly related to the question of what is the best configuration of trackers in a given terrain to minimize mutual shading and the cover-to-ground ratio, i.e., is it better to install more PV panels and have more shadows or is it preferable to have fewer PV panels hence less shading? These questions are further extended and detailed in Chapter 2. To summarize, a simple and generic method was developed to simulate a large PV plant and provide a complete profile of the shadows cast in each tracker along

each day of the year. The developed method took advantage of popular ray-tracing software which simplifies the computation of shadows between mutual PV trackers or obstacles, by simply modeling the panels and running a script to compute the shadows for every sun position in the sky during the year (for a given location) . This study resulted in a scientific publication in the form of a paper in a scientific magazine, included in Chapter 2 [11].

Regarding the second research question, there are many ways to interconnect two (or more) different power generators (with different or same energy sources). The most natural combination is to use a stable energy source with a less stable one or to use some kind of storage system to directly store electricity. Regarding the mix of PV power with another source, an interesting opportunity arose. The University of Évora (institution where this thesis was developed) is located in the interior and south of Portugal, close to Spain. This region is rich in solar radiation and has a lot of agro-industries which provide the perfect conditions to implement a less explored hybrid combination: biogas and solar (PV) energy. Near Badajoz, Spain, there was a project to build a biogas power plant that used the residues of local pig slaughterhouses to produce biogas to then produce electricity. The projected power plant had a very large parking lot, which could be covered with a PV plant to obtain a more stable and predictable power output. The PV power would be primarily used (either for operational needs or to sell to the grid) and then the remaining power would be provided by the biogas. This way, this hybrid system could store energy (biogas) as when the PV plant was producing electricity, less biogas was necessary so the remainder of it could be stored in tanks or inflatable holders. This study about the hybridization of a biogas power plant with a PV plant resulted in a scientific publication in a specialty journal, included in Chapter 3 [12].

- Chapter 2 - "Simulation and computation of shadowing losses of direct normal solar radiation in a photovoltaic field with multiple 2-axis trackers", [11].
- Chapter 3 - "Energy self-sufficiency through hybridization of biogas and photovoltaic solar energy: an application for an Iberian pig slaughterhouse", [12].

1.1.3 The following work

The last research question was approached as part of a European project called PVCROPS. This project aimed specifically to solve current problems in PV technology regarding reliability, prediction and mitigation of related problems. The main responsibility of UEVORA in this project was to test the suitability of new state-of-the-art batteries (Vanadium Redox Flow and Lithium-ion) with energy management strategies developed specifically for PV plants and BIPV. Two real size prototype

systems were built (one for each battery) to validate and improve the EMS only tested in simulations with experimental data and test the suitability of each battery for these specific applications. The prototypes were composed of a PV system connected to a battery that was in turn connected to a building and/or to the public electrical grid, where they were assembled and installed. The construction, programming and initial operation of the batteries is described in Chapter 4. The following work regarding EMS testing and validation resulted in one oral presentation [14], three conference posters [15, 16, 17] (in Annex) and a journal paper ([13]) included in Chapter 5.

Other task performed for PVCROPS project was the revision and translation of a manual of good and bad practices for the installation of BIPV and PV plants, developed by the PVCROPS partners. The final document was presented as a poster in the 2013 European Photovoltaic Solar Energy Conference and Exhibition, in Paris, France, and was later published in the proceedings (see Annex) [18].

- Chapter 4 - "Construction, programming and operation of two state-of-the-art Vanadium Redox Flow and Lithium-ion batteries"
- Chapter 5 - "Implementation and validation of a Self-Consumption Maximization energy management strategy in a Vanadium Redox Flow BIPV demonstrator", [13].

1.2 Structure of the PhD thesis

This PhD thesis is structured as follows:

- Chapter 1: Background and general motivation
- Chapter 2: Study of shadowing losses in PV plants using simulations done in a commercial ray-tracing software
- Chapter 3: Study of the hybridization of a biogas power plant by incorporating a PV plant and use the biogas as energy storage
- Chapters 4: Construction, programming and operation of two state-of-the-art Vanadium RF and Lithium-ion batteries
- Chapter 5: Implementation and validation of a Self-Consumption Maximization energy management strategy in a Vanadium Redox Flow BIPV demonstrator
- Chapter 6: Future perspectives and lines of investigation
- Chapter 7: Conclusions

- Annex: Additional material

Bibliography

[1] International Energy Agency (IEA), *Key World Energy Statistics 2015*, 2015, pp. 1-81

[2] World Health Organization (WHO), *World Health Statistics 2016: monitoring health for the SDGs, sustainable development goals*, 2016, pp. 1-136

[3] Trigg, T., Telleen, P., Boyd, R., Cuenot, F., *Global EV Outlook: Understanding the Electric Vehicle Landscape to 2020*, 2013, pp. 1–41

[4] Feldman, D., Barbose, G.; Margolis, R.; James, T., Weaver, S., Darghouth, N., Fu, R., Davidson, C., Booth, S, Wiser, R., *Photovoltaic System Princing Trends: Historical, Recent and Near-Term Projections*, 2014, pp. 1-32

[5] Solar Power Europe, *Global Market Outlook, For Solar Power 2015-2019*, 2015, Available online: `http://www.solarpowereurope.org/insights/global-market-outlook/` (accessed on 11^{th} April 2016)

[6] Marcos, J., Marroyo, L., *Smoothing of PV power fluctuations by geographical dispersion*, 2012, Progress in Photovoltaics: Research and Applications 20, pp. 226–237

[7] Patsalides, M., Stavrou, A., Efthymiou, V., Georghiou, G. E., *Towards the establishment of maximum PV generation limits due to power quality constraints*, 2012, Int. J. Electr. Power Energy Syst. 42, pp. 285–298

[8] Wang, G., Ciobotaru, M., Agelidis, V. G., *Minimising output power fluctuation of large photovoltaic plant using vanadium redox battery storage*, 2012, IET Conf. Publ. , D41.

[9] Executive Office of the President of the United States, Council of Economic Advisers, *Incorporating renewables into the electric grid: Expanding opportunities for smart markets and energy storage*, 2015, Available online:`https://www.whitehouse.gov/sites/default/files/page/files/20160616_cea_renewables_electricgrid.pdf` (accessed on 20^{th} June 2016)

[10] Wolfe, S., Mensah, A., *Overcoming Challenges to High Penetration of Solar PV: Using Optimized Energy Storage and Distribution Grid Controls*, 2012, Electr. J. 25, pp. 43–47

[11] Fartaria, T., Collares Pereira, M., *Simulation and computation of shadow losses of direct normal, diffuse solar radiation and albedo in a photovoltaic field with multiple 2-axis trackers using ray tracing methods*, Solar Energy 91 (2013), pp. 93-101

[12] González-González, A., Collares Pereira, M., Cuadros, F., Fartaria, T., *Energy self-sufficiency through hybridization of biogas and photovoltaic solar energy. An application for an Iberian pig slaughterhouse*, 2014, Journal of Cleaner Production 65, pp. 318-323

[13] Fialho, L., Fartaria, T., Narvarte, L., Collares Pereira, M., Implementation and Validation of a Self-Consumption Maximization Energy Management Strategy in a Vanadium Redox Flow BIPV Demonstrator, 2016, Energies 9(7): 496, doi:10.3390/en9070496

[14] Fialho, L., Fartaria, T., "Demonstrators of Li-ion and Vanadium Redox Batteries", Oral Presentation, European Photovoltaic Solar Energy Conference and Exhibition (2015), Parallel event: "PV CROPS: Novel solutions for a high PV penetration in EU electrical networks with lower LCOE."

[15] Fialho, L., Fartaria, T., Collares Pereira, M., *Performance Characterization of a Vanadium Redox Flow Battery*, Poster presentation, European Photovoltaic Solar Energy Conference and Exhibition (2015) Hamburg, Germany

[16] Fialho, L., Fartaria, T., Collares Pereira, M., *Validation of a Energy Management Strategy for a BIPV System with a Vanadium Battery Demonstrator*, Poster presentation, European Photovoltaic Solar Energy Conference and Exhibition (2015) Hamburg, Germany

[17] Fialho, L., Fartaria, T., Collares Pereira, M., *Validation of a Energy Management Strategy for a BIPV System with a Lithium Ion Battery Demonstrator*, Poster presentation, European Photovoltaic Solar Energy Conference and Exhibition (2015) Hamburg, Germany

[18] Martinez Moreno, F., Helleputte, F., Tyutyundzhiev, N., Rabal Echeverria, D., Conlon, M., Fartaria, T., Oteiza, D., *Good and bad practices in pv plants.*,European Photovoltaic Solar Energy Conference and Exhibition (2013) Paris, France, pp. 1-3.

Chapter 2

Simulation and computation of shadowing losses of direct normal solar radiation in a photovoltaic field with multiple 2-axis trackers[†]

Abstract

A method is presented to simulate and compute shadow losses of direct normal solar radiation in a PV field with multiple 2-axis trackers using a raytracing software. This method is simple and precise and can be used to calculate losses of a very large number of trackers with any kind of PV panel, either traditional PV or concentrated photovoltaic panels. By reducing the problem to a representative sample of the different trackers in the field and studying each tracker individually, the simulations can be done very fast and with great precision. A case study is performed to show the application of the method.

Keywords: shadow losses, d.n.i., 2-axis tracker

Nomenclature

C	Concentration
CPV	Concentrated PhotoVoltaics
$d.n.i.$	Direct normal irradiance
PV	PhotoVoltaics
STE	Solar Thermal Electricity

[†]Tomás Oliveira Fartaria[a,], Manuel Collares-Pereira[a], Simulation and computation of shadowing losses of direct normal solar radiation in a photovoltaic field with multiple 2-axis trackers, Solar Energy 91, 93-101, 2013.

[a]Universidade de Évora, Largo dos Colegiais 2, 7004-516 Évora, Portugal

F_{GS}	Geometrical Shadow Factor
N_{SB}	Number of shaded blocks
N_{t}	Number of time intervals used in the simulations
trk	Tracker

2.1 Introduction

One of the factors affecting electricity production in PV systems with multiple trackers is mutual shading. In this paper, the term "trackers" refers to the set tracker plus the PV modules installed on it. In systems with multiple trackers the use of land has an associated cost. Attempting to reduce costs by bringing the trackers closer together, will increase mutual shading generating unwanted losses [1]. Besides, tracker distribution and proximity has also another impact on system cost, that associated with cable length. Thus, a method to calculate the losses associated to mutual shading is important for a final cost optimization at the stage of field design.

Mutual shading results from the relative positions of the surfaces (PV system entrance aperture on each tracker) tracking the (apparent) motion of the sun and thus it differs from hour to hour on each day and from day to day.

There are several commercial softwares for shadow losses calculations (as, for instance, PVSYST[2], Shadow Analyzer[3], Shadow FX[4], PV*Sol[5], etc). The user typically pays for access and finds out that these tend not to be directly or easily applicable, as they are often developed for the calculation of shadows generated by buildings and other static objects and hard to automate for situations involving continuously varying conditions. Others show only shadows projected on the ground and on other objects, but do not give quantitative answers.

There are also algorithms (for instance as in [1], [6], [7]) which calculate shadow losses by using trigonometric formulae to find out shadow sizes and then superimpose those for different positions of the sun in the sky.

There are also algorithms embedded in software used for the definition and sizing of heliostat fields in, for instance, Central Receiver Tower STE systems, precisely to evaluate shadowing and blocking losses, but again these are not easily or directly available to the PV systems engineer.

In this paper a simple method is presented for the calculation of shadowing losses in 2-axis tracking PV collector fields, with conventional PV modules or with PV cells combined with concentration optics (CPV), usually lenses or mirrors concentrating many hundreds of times d.n.i. solar radiation on very efficient multi-junction solar cells [8], [9]. Using a raytracing software, modeling the photovoltaic field is done

in a very simple way, enabling a very precise reproduction of the complete field, even when it includes static/moving obstacles and different tracking heights due to terrain irregularities.

Shadows cast at the end (or beginning) of the day are not as important as those occurring at midday, simply because the corresponding amount of available energy being lost is much smaller. Thus the kind of loss calculation that matters should be energy weighted, as proposed in this paper. The paper proposes the use of annual average hourly d.n.i. data for any given location where the PV collector field is installed.

At present this data is not widely available from genuine long term measurements on location, but several hourly radiation sequence generation methods area available for any specific location, interpolating/extrapolating from the few locations that have available measurements [10], [11], [12], [13], [14].

2.2 Problem description

A large PV collector field is composed by several 2-axis trackers on which simple PV panels or CPV systems are mounted, as schematically depicted in Figures 2.1. 2 – axis trackers maximize energy collection by keeping PV system always perpendicular to the sun's rays. If the trackers are assembled too close to each other, one tracker standing in front of another in respect to the sun's position in any given instant, may cast a shadow on the tracker behind, reducing its electricity production (as depicted in Figure 2.2). In order to correctly predict the amount of energy produced by the complete collector field it is necessary to be able to compute the amount of solar radiation lost due to shading at any given hour of the day.

The shading loss calculation per tracker on an yearly average can be done according to the energy weighted formula (equation 5.3),

$$Shadowing\ Losses[trk] = \frac{\sum_{t=1}^{Nt} Irradiance[t] * Shadow\ Factor_{trk}[t]}{\sum_{t=1}^{Nt} Irradiance[t]} \tag{2.1}$$

where "Nt" stands for the number of time intervals that the year was divided (8760 for hourly calculations or 525600 for 10 min intervals). Irradiance[t] is the d.n.i. value corresponding to each time interval (t) and Shadow Factor$_{trk}$ is defined according to [15], where an accurate, but empirical formula, was suggested for it: the geometrical shadow factor, F_{GS}, is the ratio of a area divided by the total surface area of each

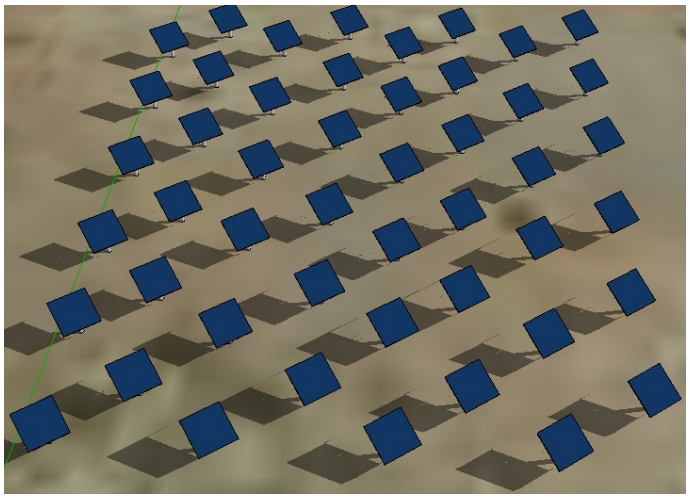

Figure 2.1: Example of PV collector field with multiple trackers.

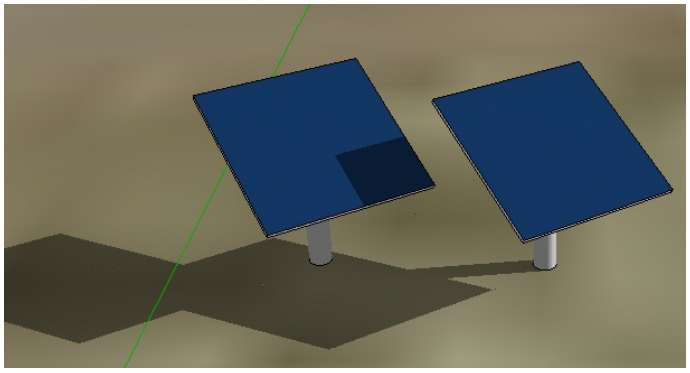

Figure 2.2: Example of shading on a certain hour.

tracker, is multiplied by the ratio of the number of shaded blocks (N_{SB}), to that number incremented by a factor 1 one (N_{TB}+1), yielding the so called effective shadow factor (hereby named simply Shadow Factor for simplification) (equation 5.4):

$$Shadow\ Factor[trk] = (1 - F_{GS}) * \left(1 - \frac{N_{SB}}{N_{TB} + 1}\right) \tag{2.2}$$

It should be noted that there is no need to know the details of the optics or of the cell conversion efficiency, since the resulting values would figure both in the numerator and denominator of the energy weighted fraction.

An example from CPV explains more clearly what is meant: the system mounted on the tracker is an ensemble of concentrating optics, each associated with its multijunction cell. These cells are grouped in series /parallel set of connections and a set of bypass diodes. For the purpose of the paper a set of cells protected by the same bypass diode constitutes a block. The number of cells existing in each block is different from case to case. In PV panels, modules typically integrate 20 to 24 individual cells, as for CPV systems all cells possess a bypass diode, resulting in one

module per cell. The effect of module shadowing is here considered in two extreme situations (as was done by Garcia et al. [15]): the most favorable case where power loss is considered equal to the Shadow Factor, and the worst case where the slightest shadow will result in zero production from the cell.
The difficulty of the calculation is associated with the fact that for each time interval it is necessary to calculate the shadows being cast by the surrounding trackers, all continuously following the sun and thus constantly altering their position on the horizon on any given tracker.
A traditional calculation of projected shadows is a cumbersome process requiring long computational time, since beyond the calculation of the shadowed areas, it is necessary to associate those to each block and only then calculate the shadow factor. One way to simplify matters is to use a ray tracing software, with a relatively large number of rays (to be determined or varied according to the number of trackers and of blocks on each of the trackers) allowing for a quick and precise simulation of the PV system.

2.3 Methodology

The procedure explained below was optimized to be applied to PV collector field with 2-axis trackers (with some minor changes in the raytracing configuration, this method can be applied to 1-axis and even fixed PV collectors), but it takes only d.n.i. solar irradiance into consideration. This fact deserves a further comment, since there is also diffuse solar irradiation getting to the PV system surface. In the case of a CPV system this omission is quite understandable, since any concentrating optics of geometrical concentration factor of C, can only collect 1/C of the incident diffuse radiation [16], therefore this is really a non-existing problem. However for conventional (non-concentrating) PV systems that deserves a further comment, since diffuse radiation can easily represent 30% of the total available radiation. However, in this case, what happens is indeed a continuous change of the amount of diffuse radiation being blocked by the trackers on the "horizon" of each individual tracker; but given the typical distances between trackers, and the fact that this blocking tends to happen for large angles of incidence corresponding to very little absorption by the system, anyways, it is justifiable to neglect what would be a truly small effect.
A PV collector field with multiple trackers is sometimes integrated by hundreds of units. Individually evaluating shadow losses for each one of them would be cumbersome and would take time on regular machines. One way to handle this is to choose a sample of trackers representing the whole collector field. This sample should contain

trackers "types" representing all the different situations trackers have in the collector field, as, for instance, those that are on the field edges, surrounded by other trackers in all directions, etc. in such a way that any tracker in the sample corresponds to one or more tracker "type" in the collector field. Calculations are then done for each tracker type and the final result is simply obtained by multiplying each result by the corresponding number of like trackers in the field and adding it all at the end. For each tracker in the sample a model is made to be introduced in a raytracing program. Trackers are modeled as rectangular detectors coinciding with the full active radiation collecting surface on the tracker.
In turn these rectangles are divided into pixels corresponding to the number of blocks defined above, i.e., in the simulation software pixels will simulate (are equivalent to) blocks. Detectors are defined as perfect absorbers so that full blocking is guaranteed when shading happens. The sun is defined as a rectangular source which emits radiation perpendicularly to the surface, towards the detector being studied, and emitting parallel rays. Rotating the surfaces is the same as rotating the sun. A coordinates rotation matrix is used according to the zenith and azimuth hourly angles. A total amount of arbitrary power is homogeneously distributed in such a way that each pixel gets the same number of rays as any other unshaded neighboring pixel. The number of rays should be high enough to provide any predefined accuracy for the result. The source is not defined as large enough to accommodate at the same time all the trackers simultaneously, as in that way, most of the rays pass in between the trackers and would not be used for the calculation. In fact the trick is to use a source with just the right size of each tracker, since 2-axis tracking automatically guarantees that all rays leaving the source will fall on the tracker being studied, except when it is being shaded by another tracker. As the source has the same area as the detector, perfect tracking guarantees that detector area seen by the source is always the total area. In this way dividing the power from the source by the number of pixels, yields the power arriving per pixel. Thus the individual Shadow Factor for each pixel is obtained by relating the power absorbed per pixel for each zenith/azimuth configuration to the total power that pixel would collect in an ideal situation (no other trackers present). Adding up this result for all pixels in a tracker a final value for the shadow factor for the tracker being studied, Shadow Factor$_{trk}$, results for that configuration. Proceeding likewise for all configurations zenith/azimuth pairs yields the shadow factor for the tracker being studied for all hours along the year. The calculation routine can be summarized in the following way:

1. Establish relative positioning of the trackers in the representative sample through the (3D) coordinates of the surface center on each tracker;

2. Create a list with sun's zenith and azimuth angles corresponding to every hour from sunrise until sunset, for each day of the year;

3. Using the previous list, a pair of azimuth and zenith angles is chosen to change the trackers and sun's inclination.

4. Launch the raytracing. For each tracker at a time a cycle is performed to read the radiation absorbed by each pixel. If the value is above cutoff (defined as the maximum percentage of shaded block to consider the block as active (producing energy)) times the maximum radiation per pixel, the variable responsible for the number of active pixels is incremented;

5. to allow for a complete and later tracker analysis the data for shadow factor as a function of zenith and azimuth angle pairs are saved in a file;

6. With the data obtained, shadow losses are computed by simply multiplying the d.n.i. value of each 10min interval to the respective shadow factor, for the entire year;

7. To finally compute the global shadow factor of the PV field, an weighted average is performed by multiplying the number of trackers in the PV field equal to a tracker in the sample by the respective shadow factor, for every tracker in the sample (equation 5.5.

$$Global\ shadow\ factor = \frac{\sum_{trk=1}^{n} Shadow\ factor[trk] * Number\ in\ field[trk]}{\sum_{trk=1}^{n} Number\ in\ field[trk]} \tag{2.3}$$

2.4 Case study

A calculation was made for the system shown in Figures 2.3 and 2.4 using d.n.i data for one year in Faro, Algarve, Portugal (latitude 37°). Tracker and Field details:

- dimensions of the tracking surface: length : 8.536m ; width 6.515m, height of the central point 2.7m;
- each tracking surface is divided into 24*18 pixels;
- the space between trackers in the terrain is : N-S 17 m and E-W 21 m;
- tilt angle of the terrain : two cases were considered, 0° and 3.4° due South;

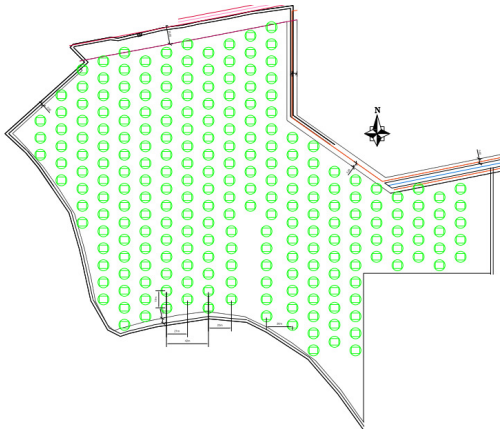

Figure 2.3: Terrain configuration and lay out of large PV field: each green circle represents a PV system (tracker + PV modules).

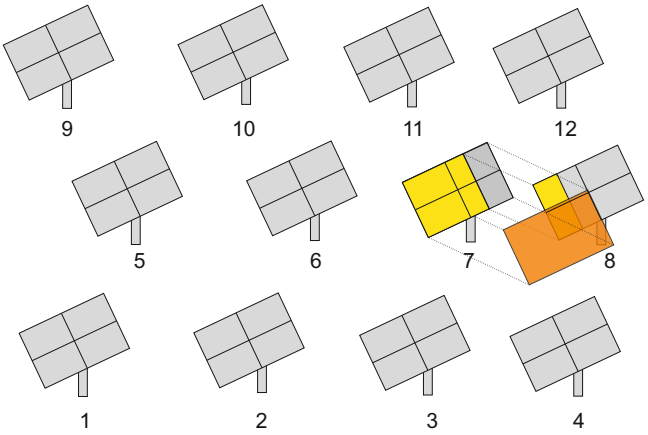

Figure 2.4: Representative sample of large PV field; gray rectangles represent the PV systems (detectors). The orange rectangle represents the sun (source), and the yellow parts are illuminated areas; darker gray indicates a shadowed area.

The PV field was reduced to a representative sample comprising 12 trackers. Figure 2.3 shows the terrain configuration and the tracker's distribution. Figure 2.4 depicts the representative sample.

Several working parameters were chosen for the performance simulation:

- 5000 rays
- The power associated with the set of rays was arbitrarily set at 10kW; this value should guarantee that the power per ray is above the number of significant

decimal places established by the software. Per example, using a software with 2 decimal places to measure the power hitting the detector, using 50000 rays per simulation, each ray should correspond to at least 0.01 W, which means the global energy of the source should be at least 0.01*50000 = 500W.

2.4.1 Results

The results obtained for the average losses due to shading for each of the trackers in the sample are listed in table 2.1. Calculations were performed considering two cutoff levels (maximum percentage of shaded block to consider the block as active (producing energy)); one pessimistic (0.99) in which any shadow will nullify the power produced by the shaded block, and an optimistic case (0.01) in which the amount of power lost due to shading is proportional to the shaded area of the block. This approach gives a maximum and a minimum for shading results, as it was done in [7]. The final sum for the full field is also included. Two terrain tilts (β) due south are considered.

Table 2.1: Results obtained for each PV system of the representative sample (represented in Figure 2.4) for two cases: one with a leveled terrain, and the other with an inclination of approximately 3.4°, to South. Each case was subdivided in two more cases depending on the cutoff level. The last column shows the result of a weighted average performed to the large PV field.

β	**cutoff**	**1**	**2**	**3**	**4**	**5**	**6**	**7**	**8**	**9**	**10**	**11**	**12**	**total**
0°	0.01	0.51	3.50	3.83	3.37	0.50	3.50	3.83	3.37	0.51	0.02	3.84	0.35	**3.20%**
	0.99	0.76	4.74	5.06	4.36	0.76	4.75	5.07	4.37	0.76	0.05	5.08	0.41	**4.31%**
3,4°	0.01	0.37	2.86	3.19	2.86	0.37	2.86	3.19	2.86	0.36	0.02	3.19	0.35	**2.62%**
	0.99	0.57	3.74	4.05	3.55	0.57	3.74	4.07	3.55	0.57	0.06	4.07	0.41	**3.41%**

As can be seen the results for the tilted terrain exhibit less losses as expected. Trackers on the West side show practically no losses. Such is not the case for the East side trackers. This apparently strange result is explained by the fact that an energy weighted average was calculated and there is a local tendency for early morning mists or cloudier skies, affecting d.n.i. availability.

To validate this calculation method for shadow losses, the case described in [15] was considered and results were compared. This method yielded shadow losses between 3.89% e 4.53% for the same situation and assumptions. In comparison with the result reported in [15] (3.9%), the results obtained in with the method described in this paper are closer to the those measured and also reported in [18]: about 5.1%.

2.5 Conclusions

A simple method to simulate and calculate shadow losses of d.n.i. in 2-axis tracking solar PV fields was presented and discussed.
The method is practical and easily implemented requiring only some dexterity in programing to facilitate and accelerate the calculations in different field configurations and horizon conditions.
The results obtained are in agreement with those resulting from more cumbersome methods and agree also with data obtained in real situations [15] [17] [18].
Some improvements can be made for higher accuracy, namely by modeling more precisely the solar cells response under partial illumination conditions. These improvements would be particularly important for closer tracker spacing and higher shading losses, whenever space might be at a premium and an economical optimization would be more demanding.

Bibliography

[1] Perpiñán, O., "Cost of energy and mutual shadow in a two-axis tracking PV system", Renewable Energy **43** (2012) 331-342

[2] Available online: `http://www.pvsyst.com/en/`

[3] Available online: `http://www.drbaumresearch.com/`

[4] Available online: `http://www.shadowfx.co.uk/`

[5] Available online: `http://www.solardesign.co.uk/`

[6] Narvarte, L., Lorenzo, E., "Trackingand Ground Cover Ratio", Prog. Photovolt: Res. Appl. 2008; DOI: 10.1002/pip.847

[7] Lorenzo, E., Navarte, L., Muñóz, J., "Tracking and back-tracking", Prog. Photovolt: Res. Appl. 2011; DOI: 10.1002/pip.1085

[8] Solfocus, Available online: `www.solfocus.com`

[9] Magpower, Available online: `www.magpower.pt`

[10] Meteonorm, Available online: `meteonorm.com`

[11] climData sofware from SolarGis, Available online: `www.solargis.info`

[12] Typical Meteorological Year version 3 (TMY3) from National Solar Radiation Data Base, NREL, Available online: `rredc.nrel.gov/solar/old_data/nsrdb`

[13] WRMC-BSRN, Available online: `www.bsrn.awi.de/en/home/`

[14] NASA-SEE, Available online: `eosweb.larc.nasa.gov/sse/`

[15] Martínez-Moreno, F., Muñoz, J., Lorenzo, E., "Experimental model to estimate shading losses on PV arrays", Solar Energy Materials & Solar Cells **94** (2010) 2298-2303

[16] Ari Rabl, "Active solar collectors and their applications", Oxford University Press, 1985

[17] Private communication

[18] Garcıá, M., Maruri, J.M., Marroyo, L., Lorenzo, E., Pérez, M., "Partial shadowing, MPPT performance and inverter configurations: observations at tracking PV plants.", Prog. Photovolt: Res. Appl. **16** (2008) 529–536.

Chapter 3

Energy self-sufficiency through hybridization of biogas and photovoltaic solar energy: an application for an Iberian pig slaughterhouse*

Abstract

The Iberian pig slaughterhouses constitute one of the most important economic activities of Extremadura (Spain), these industries generate large quantities of wet highly pollutant organic waste that need to be managed in an environmentally correct way. On the other hand, the tendency for the constant increase in the price of energy (electricity and fossil fuels) is progressively reducing the economic returns of these companies.

This paper presents an integrated solution to an environmental and an energy problem of the companies that generate wet waste biomass. This solution consists in the hybridization of biogas (generated by anaerobic digestion of these wastes) with photovoltaic solar energy.

In the specific case of this Iberian pig slaughterhouse the results show that the most profitable option involves the installation of an anaerobic digestion plant with an electrical power of 79 kWe and a solar photovoltaic installation of 225 kWe. The total cost of both systems is 737000 €and the project presents a Payback period (PBP) of 9 years, an Internal Rate of Return (IRR) of 9% and a Net Present Value (NPV) of 0.70 millions €.

Keywords: Hybridization, Biogas, Photovoltaic solar energy, Slaughterhouse waste, energetic benefits, economic feasibility

---

*A. González-González[a,], M. Collares-Pereira[b], F. Cuadros[a], T. Fartaria[b], Energy self-sufficiency through hybridization of biogas and photovoltaic solar energy: an application for an Iberian pig slaughterhouse,Journal of Cleaner Production 65, 318-323, 2014.

[a]Departamento de Física Aplicada, Universidad de Extremadura, Avenida de Elvas S/N, 06006 Badajoz, Spain

[b]Cátedra BES Energias Renováveis, Universidade de Évora, Casa Cordovil. Rua Dr, Joaquim Henrique da Fonseca, 7, 7000-890 Évora, Portugal

Nomenclature

AD	Anaerobic Digestion
COD	Chemical Oxygen Demand
H_0	(Extraterrestrial solar irradiation)
$Hcol$	(solar irradiation incident on the photovoltaic module)
Hd	(Diffuse solar irradiation on the Earth's surface)
Hh	(Monthly average global irradiation on a horizontal surface)
HRT	Hydraulic Residence Time
IRR	Internal Rate of Return
NPV	Net Present Value
PBP	Payback period
VDS	Volatile Dissolved Solids
VFA	Volatile Fatty Acids
VSS	Volatile Solids in Suspension

3.1 Introduction

In the Autonomous Community of extremadura, the economy is heavily dependent on food industry because both agriculture and livestock provide the basis for an industrial sector based on the transformation of these products, within a sector which highlights the importance of the meat processing industry, representing 24.8% of turnover [1].

Furthermore this industry is characterized by the generation of highly polluting waste (high organic matter and moisture content). Population and industrial growth, plus the concentration of population in large cities, causes that residual biomass generation to be so abundant and so located, that the auto-degradation capacity of the medium is insufficient and it is necessary to apply different treatment techniques to these wastes before their discharge into the natural environment. Otherwise it would generate numerous environmental problems, mainly in the water, causing eutrophication, and in the atmosphere due to the emission of greenhouse gases (methane and carbon dioxide) as a result of decomposition in uncontrolled conditions.

Currently solid wastes generated by the meat processing industry are managed by specialized companies in waste treatment that charge a fee for their collection and

disposal. The transformation is essentially a reduction in the size of the particles, and then the wastes are submitted to high temperatures, always higher than 100ºC for a period of time. After this transformation, they can be incinerated or deposited in a landfill. This method of treatment is effective but requires large amounts of energy (heat and electricity) therefore; it would be advisable to find another technique of treatment to decrease costs.

Another problem of the meat processing industry is the gradual increase in the cost of non-renewable energy. This increase in energy expenditure cannot be passed on to the final consumer, and so lowers the profit margin. This situation coupled with increasingly restrictive environmental legislation is affecting the economic feasibility of these activities.

It is an indisputable fact that the meat processing industry has problems that cannot be ignored and need quick and effective action. In this sense, the technology of anaerobic digestion (AD) provides a comprehensive solution to solve both problems: i) the search for new energy sources and ii) the reduction of the potential pollution of industrial activity, because it is a biological process in which the biodegradable organic matter, in absence of oxygen and as result of the action of a group of specific bacteria (hydrolytic, acidogenic, acetogenic and methanogenic), decomposes into a gaseous fuel called biogas (CH4, CO2, H2, H2S, etc.) which has a high calorific value and a digested effluent, which can be used as an organic fertilizer. Moreover anaerobic digestion has the advantage of being completely manageable, i.e., biogas can safely be stored to be used when it is needed, so this technology has an enormous potential for hybridization with photovoltaic solar energy for electricity generation, to allow for energy self-sufficiency of the agrifood industry.

This paper presents the results obtained by analyzing in detail the environmental and energy needs of an Iberian pig slaughterhouse called Jamón y Salud S.L. which is located in Llerena, Badajoz, (Spain) and proposes a integral solution that involves the installation of an anaerobic digestion plant designed to treat the volume of waste generated annually by this company and transform it into useful energy (biogas), complemented by a photovoltaic solar energy plant, such that together, they can completely cover the energy consumption of the slaughterhouse. Finally, we examine the economic viability of these renewable energy installations.

This work can be used as a reference for designing and evaluating the feasibility of the hybridization of biogas and photovoltaic solar energy to achieve energy self-sufficiency of any industry that generates wet organic waste.

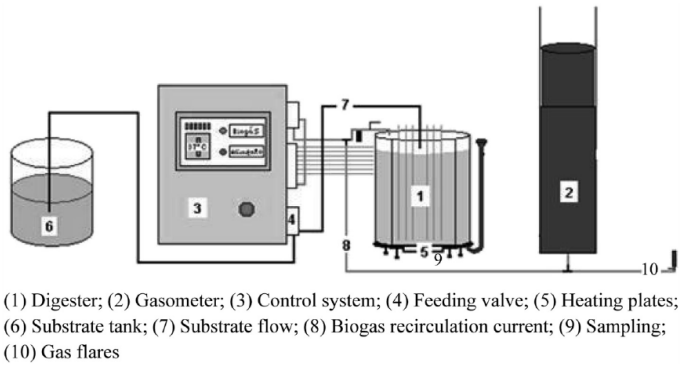

Figure 3.1: Basic scheme of the continuous flow stirred tank reactor (CSTR).

3.2 Material and methods

3.2.1 Anaerobic digestion

The AD experiments have been carried out using a continuous flow stirred tank reactor [2], Figure 3.1 shows a basic scheme of the experimental setup.

Samples were periodically taken from the digester in order to appropriately monitor the following parameters: Chemical Oxygen Demand (COD), Volatile Fatty Acids (VFA), alkalinity, pH, Volatile Solids in Suspension (VSS) and Volatile Dissolved Solids (VDS).

VFA, alkalinity, pH, VSS, and VDS were determined according to the standard methods [3, 4], whereas COD was analyzed using Nanocolor (MachereyeNagel) kits and a PF-12 portable spectrophotometer (MachereyeNagel).

In each experience a different flow was tested,which was fed for a period of twice the Hydraulic Residence Time (HRT) (Time period in which the substrate is in the reactor in contact with the bacterial population), the first HRT stands for the acclimatization period, after which the reaction stabilizes, i.e. the organic matter content is reduced down to a constant value, whereas the generated methane reaches a maximum. This way, reliable data of the degradation process and of methane production can be obtained for each of the tested flows. Once the set of designed experiments were fully conducted, the optimum flow (i.e. the value at which the highest COD reduction and methane production were achieved) was determined.

3.2.2 Economic feasibility

The economic viability of the system of renewable energetic supply that integrates anaerobic digestion and solar photovoltaic energy was analyzed based on a number

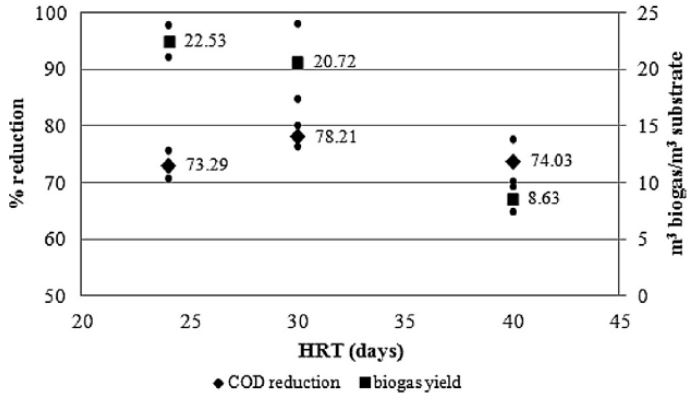

Figure 3.2: Biogas production and COD reduction of Iberian pig slaughterhouse waste as a function of HRT

of assumptions listed below:

Calculation of the electric and thermal power of the anaerobic digestion plant

In order to calculate the electric and thermal power of the AD plant it was assumed that this system operates 8000 h/year burning the biogas generated by the AD of wastes produced by the slaughterhouse. Electric and thermal efficiencies of the biogas engine were determined as 39% and 44.7% respectively, whereas calorific value of methane 31 MJ/Nm^3. Even though this parameter was somewhere else reported to reach up to 35 MJ/m^3 [5], a lower value will be considered in order to account for the most unfavorable scenario.

Installation costs

4000 V/installed kWe (ESETA France, personal communication) was assumed to assess the construction costs of the AD plant. Complementary costs ought to be considered regarding feasibility studies (10000 €) and administrative and authorization requirements (20000 €)[6]. Moreover the price of the storage of biogas in tanks flexible membrane was estimated at 1 €/m^3 and the construction costs of the photovoltaic solar energy plant was estimated at 1.70 €/Wp, (according some renewable energy companies this price usually varies between 1.5 and 2.5 €/Wp installed in systems with the characteristics considered in this paper).

Annual costs

Operation and maintenance costs for the AD plant are substantially higher than for the photovoltaic solar installation, the latter was estimated at 36 €/installed kWp (COENERSOL, personal communication). The costs of the AD plant are described bellow: Engine maintenance costs are estimated as 12.5 €/MWh electricity [7], the costs derived from the maintenance of the rest of the AD plant were assumed to be 2% of construction costs and labor cost was assumed as 12000 €/year.

Other costs to consider are those due to annual mortgage payment to pay the installation costs of both renewable energy plants. This cost was calculated considering 8% interest during 15 years.

Finally, we must consider indirect costs related to the treatment of lung wastes (1 kg per slaughtered pig) [8], 0.12 €/kg solid waste, (Jamón y Salud S.L., personal communication). Note these particular wastes are not suitable to undergo any anaerobic process since they exhibit a negative influence on AD.

Annual benefits

The economic benefits were estimated considering electricity savings (0.10 €/kWh) and savings in diesel for heating water (1.136 €/L diesel, [9]. The photovoltaic solar plant was oversized to ensure coverage of the electricity needs of the slaughterhouse, therefore there are biogas surpluses, at certain times of the year, which will be stored in order to be burned and generate thermal energy to heat water for cleaning the slaughterhouse. Moreover, benefits derived from the avoided costs of treatment of solid wastes were also considered (0.12 €/kg solid waste).

It should be noted that the AD plant consumes thermal energy in the pasteurization of blood and solid wastes and heating the slaughterhouse wastes from 15 to 38 °C and maintaining that temperature inside the reactor. But this energy consumption is lower than the residual thermal energy generated by the biogas engine, so, it was not taken into account in the energetic calculations.

Pasteurization of solid wastes and blood is accounted for by Normative CE 1774/2002 and Royal Decree 1429/2003 as compulsory. For such purpose, wastes need to be maintained at 70 °C for 60 min [10].

The above mentioned data allow us to calculate the main economic parameters (PBP, NPV and IRR). This calculation also was made considering a rate of increase in the price of electricity and diesel of 3.00 and a 2.30% respectively.

3.3 Results and discussion

3.3.1 Inventory of wastes generated at an Iberian pig slaughterhouse

Total amount of solid and liquid wastes generated annually by the Iberian pig slaughterhouse under study were estimated by taking as reference the number of pigs slaughtered in a standard year and the rate of waste generation. This information was provided by the slaughterhouse. Jamón y Salud S.L., located in Llerena (Badajoz), slaughtered 36093 Iberian pigs by 2009 and consumed 10467 m^3 of water therefore, the water consumption can be estimated as 290 L/slaughtered pig and the rate of solid wastes that could be treated by AD techniques was 16 kg/slaughtered pig. Moreover, according to [11] the blood content of a pig ranges between 3% and 4% of its live weight, although only between 40% and 60% of blood volume of the living animal can be recovered during bleeding operations. The volume of blood generated by pig slaughtering was therefore determined as 1.5% of its live weight, i.e. 2.3 L blood/slaughtered pig (provided mean live mass of a pig was reported as 154 kg).

These three types of waste (solid waste, blood and waste water) will be treated by AD in the same proportions in which they are generated in this slaughterhouse. It is very important to respect the proportions, since the composition of the substrate has a major influence on biogas yields.

3.3.2 Anaerobic digestion experiments

Experiments were designed with the objective of determining the optimum HRT for the Iberian pig slaughterhouse waste (regarded as the feeding substrate flow into the biodigester which allows maximum biogas production and maximum reduction in COD).

Three experiences of anaerobic digestion in continuous mode were performed in which different feeding flows were tested, 150, 200 and 250 mL substratum/day, corresponding with HRT of 40, 30 and 24 days respectively, without showing any of them signs of inhibition. In Figure 3.2, which shows the results obtained, we can observe an increase in the production of biogas as HRT decreases, reaching a maximum production of 22.53 $\pm$ 1.4 m^3 biogas/m^3 substrate (75% of methane in the biogas), with a HRT of 24 days. On the other hand, the degradation level of the substrate increases substantially when the HRT decreased to 30 days but decreases, reaching a value similar to the initial one, by treating the substrate with a HRT of 24 days.

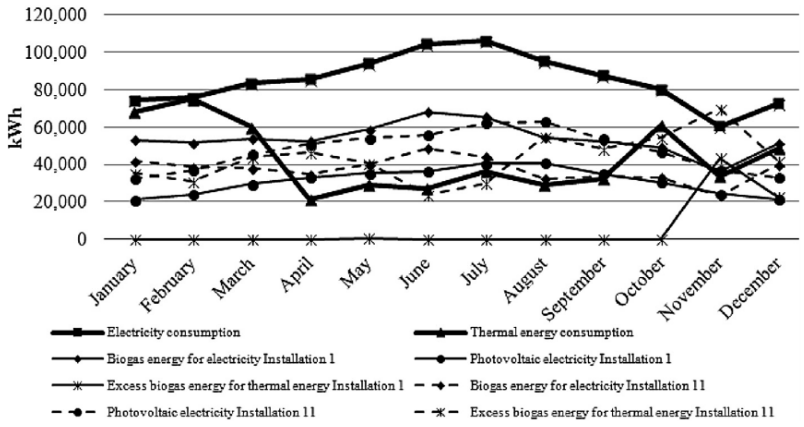

Figure 3.3: Monthly energy balances for anaerobic digestion plant and photovoltaic installations 1 and 11.

Table 3.1: Dimensions of the main components of the anaerobic digestion plants.

	Volume (m^3)	Height (m)	Diameter (m)
Pasteurization tank	4.5	2	1.7
Crushing tank	4	2	1.6
Mixing tank	174	5	7
Anaerobic digester	1000	8	12.7
Digested sludge tank	100	3	6.6
	Electric power (kWe)		Thermal power (kW_{th})
Biogas engine	78.93		90.47

Although the percentage of COD reduction is lower when the substrate is treated for 24 days ($73.29 \pm 2.49\%$), this HRT is considered optimal because it allows obtain a 8.75% more of biogas and reduce the time required for AD in 6 days, which favors the economic profitability of the AD project. Therefore, the laboratories data taken into account for the design of the anaerobic digestion plant are the obtained with a HRT of 24 days.

3.3.3 Design and sizing of the anaerobic digestion plant

Once the technical feasibility of anaerobic digestion of Iberian pig slaughterhouse waste was tested and the annual amount of solid and liquid wastes that should be treated were estimated, the necessary information was available for sizing the anaerobic digestion plant to treat these wastes. The dimensions of the main Table 4 components are shown in Table 3.1. The biogas storage will be sized later when storage needs to ensure energy supplies are known.

Table 3.2: Monthly energy consumption of the slaughterhouse Jamón y Salud S.L.

Month	Electrical energy (kWh)	Thermal energy (L diesel)
January	74,111	6825
February	75,489	7500
March	83,236	5991
April	85,332	2133
May	93,838	2903
June	104,358	2700
July	105,954	3632
August	95,348	2913
September	87,327	3228
October	80,004	6116
November	60,294	3370
December	72,714	4850
Total	1,018,005	52,162

3.3.4 Estimate of the energy requirements of an Iberian pig slaughterhouse

Requirements of electrical and thermal energy that present the Iberian pig slaughterhouse in a typical year have been studied by analyzing energy bills, daily data of electricity consumption. They are available in detail, but in Table 3.2 we only indicate monthly data in order to simplify.

The slaughterhouse Jamón y Salud S.L. consumes annually 1 million kWh of electricity, the anaerobic digestion plant can only provide 68% of this energy, therefore it is necessary to size a solar photovoltaic plant to ensure the energy self-sufficiency of this company.

3.3.5 Design and sizing of the solar photovoltaic installation

At the start of a solar photovoltaic installation design is essential to know the solar irradiation which is daily incident on the photovoltaic modules installed with a certain orientation and inclination in the area under study (Hcol), it was calculated following the procedure described by Collares Pereira [12], which builds on the data of monthly average total solar irradiation incident on a horizontal surface (Hh) in Badajoz (nearest town to the slaughterhouse from which data are available) [13], and the inclination (equal to the latitude of the place, 38.23º) and orientation (south) at which the photovoltaic modules will be installed in a very large parking area, free of objects that can cast shadows, owned by the slaughterhouse Jamón y Salud S.L. The results obtained are shown in Table 3.3.

Table 3.3: Calculation of solar irradiation incident on an inclined surface (Hcol) at 38.23º in Badajoz from daily horizontal radiation (Hh) experimental data. Data in bold identify the input data (Hh: Daily horizontal radiation) and the final data Hcol: Solar Irradiation incident on an inclined surface).

Month	Hh (MJ/m^2)	H_0 (MJ//m^2)	Hd (MJ//m^2)	Hcol (kWh//m^2)
January	**6.5**	16.237	1.344	**3.330**
February	**10.0**	21.450	2.371	**4.202**
March	**13.6**	28.220	3.593	**4.676**
April	**18.7**	34.902	5.409	**5.406**
May	**21.8**	39.680	6.745	**5.571**
June	**24.6**	41.784	7.791	**5.922**
July	**25.9**	40.750	7.977	**6.391**
August	**23.8**	36.938	6.972	**6.479**
September	**17.9**	30.710	4.910	**5.709**
October	**12.3**	23.480	3.064	**4.804**
November	**8.2**	17.545	1.817	**3.943**
December	**6.2**	14.667	1.252	**3.395**

Table 3.4: Characteristics of the solar photovoltaic installations.

Plant PV #	Number of PV modules	Photovoltaic power (kWp)	Plot Size (m) Wide	Long	Area (m^2)	Biogas storage to electricity (m^3)	Biogas storage to heat (m^3)	Total biogas storage (m^3)
1	821	205.25	43.4	53	2300	9000	1900	10,900
2	860	215	45.6	53	2417	7300	2300	9600
3	870	217.5	44.9	54	2425	6900	2500	9400
4	880	220	46.3	53	2454	6600	2600	9200
5	890	222.5	46.7	53	2475	6300	2700	9000
6	900	225	47	53	2491	6000	2800	8800
7	950	237.5	49.9	53	2645	4900	3400	8300
8	1000	250	53	53	2809	3900	4000	7900
9	1100	275	56.3	55	3097	2400	5100	7500
10	1200	300	57	60	3420	1200	11,300	12,500
11	1261	315.25	60.4	60	3624	900	19,100	20,000

Moreover it is very important to know the technical characteristics of the photovoltaic modules to be used in the photovoltaic system: They are stationary modules made of monocrystalline silicon with an area of 1.66 m^2 and a yield of 15% (value that take into account energy losses due to dirt, high temperatures, etc.). Based on data of monthly average solar irradiation incident on the photovoltaic plant and the characteristics of the photovoltaic modules to be installed, several photovoltaic plant sizes were considered, one of them to ensure the coverage of the requirements of electrical energy, and the excess biogas will be used to generate heat and avoid the consumption of certain amount of diesel (installation 1), another one to ensure the coverage of the requirements of electrical and thermal energy (installation 11) and another with intermediate power between 1 and 11.

The slaughterhouse under study presents a continuous electricity consumption during daylight and it is higher than photovoltaic power generation, therefore, photovoltaic power not need to be stored. It was decided store the biogas since its storage is substantially cheaper. Moreover, it should be noted that biogas storage has been oversized to ensure the coverage of energy needs and avoid that any amount of biogas is wasted. Table 3.4 shows the characteristics of these solar photovoltaic installations. It is noteworthy that when the photovoltaic installed power is increased the volume of storage of biogas for electricity is decreased and the storage of gas for heat is increased. This is due to the fact that the increase in photovoltaic installed power increases the percentage of electricity generated from this renewable source, so that a smaller volume of biogas is required to generate electricity and the excess biogas is stored to generate thermal energy.

Additionally, Figure 3.3 shows the monthly energy balances of the anaerobic digestion plant along with photovoltaic installations 1 and 11. The energy balances were made considering daily data decomposed in hourly data, but monthly balances are presented to simplify. These balances show that the biogas storage sized can cover the electricity supply and part of the requirements of thermal energy of the Iberian pig slaughterhouse with the photovoltaic installation 1 and the total requirements of electric and thermal energy with the photovoltaic installation 11.

3.3.6 Economic feasibility of the hybridization of biogas and photovoltaic solar energy

The main economic parameters for the two main proposed solutions have been calculated considering the calculations assumptions explained in section 2.2 and the technical characteristics of the anaerobic digestion plant and the photovoltaic system (1 and 11). The detailed economic analyses are shown in Tables 3.5 and 3.6.

Moreover, if we perform a sensitivity analysis, we would determine which of

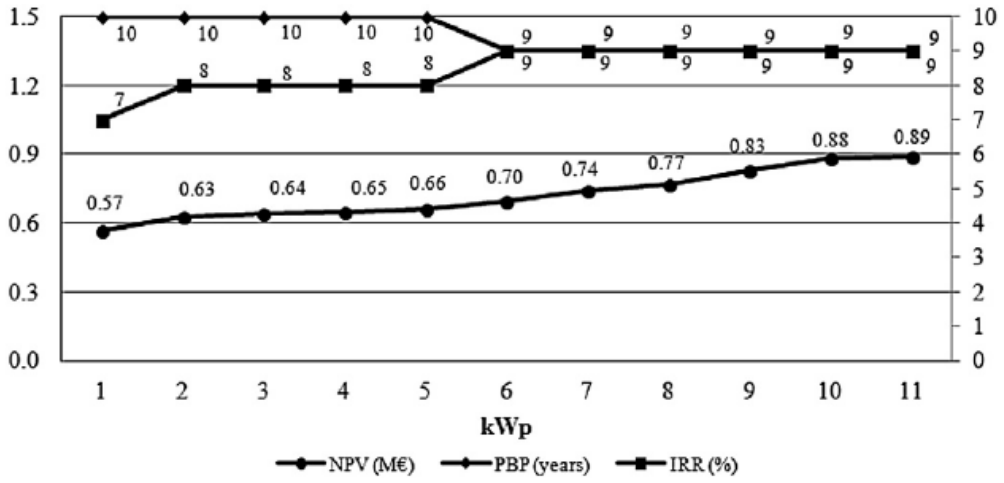

Figure 3.4: Sensitivity analysis of renewable energy installations in terms of the photovoltaic power installed.

Table 3.5: Detailed economic analysis of the anaerobic digestion plant and the photovoltaic installation 1.

Year	Income				Cost	Benefits	Cash flow
	Electricity savings	Saving diesel	Saving in waste management	Total income			
0						-705,545	-705,545
1	101,762	7638	69,299	178,698	119,487	59,212	-646,333
2	104,814	7814	69,299	181,927	119,487	62,440	-583,893
3	107,959	7994	69,299	185,251	119,487	65,764	-518,129
4	111,198	8178	69,299	188,674	119,487	69,187	-448,942
5	114,533	8366	69,299	192,198	119,487	72,711	-376,231
6	117,969	8558	69,299	195,826	119,487	76,339	-299,891
7	121,509	8755	69,299	199,562	119,487	80,075	-219,816
8	125,154	8956	69,299	203,409	119,487	83,922	-135,894
9	128,908	9162	69,299	207,369	119,487	87,883	-48,011
10	132,776	9373	69,299	211,447	119,487	91,961	43,949
11	136,759	9589	69,299	215,646	119,487	96,159	140,109
12	140,862	9809	69,299	219,969	119,487	100,483	240,591
13	145,088	10,035	69,299	224,421	119,487	104,934	345,525
14	149,440	10,266	69,299	229,004	119,487	109,518	455,043
15	153,923	10,502	69,299	233,724	119,487	114,237	569,280
						PBP (years)	10.00
						IRR (%)	7
						NPV (€)	569,280

Table 3.6: Detailed economic analysis of the anaerobic digestion plant and the photovoltaic installation 11.

Year	Income				Cost	Benefits	Cash flow
	Electricity savings	Saving diesel	Saving in waste management	Total income			
0						-901,645	-901,645
1	101,762	59,285	69,299	230,345	145,935	84,410	-817,235
2	104,814	60,648	69,299	234,761	145,935	88,826	-728,409
3	107,959	62,043	69,299	239,300	145,935	93,365	-635,044
4	111,198	63,470	69,299	243,966	145,935	98,031	-537,013
5	114,533	64,930	69,299	248,762	145,935	102,827	-434,186
6	117,969	66,423	69,299	253,691	145,935	107,756	-326,430
7	121,509	67,951	69,299	258,758	145,935	112,823	-213,607
8	125,154	69,514	69,299	263,966	145,935	118,031	-95,576
9	128,908	71,113	69,299	269,320	145,935	123,385	27,809
10	132,776	72,748	69,299	274,823	145,935	128,887	156,696
11	136,759	74,422	69,299	280,479	145,935	134,544	291,240
12	140,862	76,133	69,299	286,293	145,935	140,358	431,598
13	145,088	77,884	69,299	292,270	145,935	146,335	577,934
14	149,440	79,676	69,299	298,414	145,935	152,479	730,413
15	153,923	81,508	69,299	304,730	145,935	158,795	889,208
						PBP (years)	9.00
						IRR (%)	9
						NPV (€)	889,208

the photovoltaic plants achieves the best economic profitability. In light of Figure 3.4 optimal choice would opt for the construction of a photovoltaic solar plant of 225 kWp, because it achieves the lowest Payback time (PBP, the time required to recover the investment), 9 years, and the highest net present value (NPV, i.e. the money that the owner can get at the end of the project, after 15 years) and the internal rate of return (IRR, interest rate on investment), which were determined as €0.70 million and 9%, respectively.

3.4 Conclusions

This paper demonstrates that there is a very good reason to encourage the implementation of renewable energy systems in the agrifood industry and it is possible to reach an environmentally correct management of wet organic waste through anaerobic digestion since the results obtained and the economic studies indicate that it is technically feasible and cost effective to achieve energy self-sufficiency in an Iberian pig slaughterhouse by hybridization of biogas with photovoltaic solar energy.

3.5 Acknowledgments

This work was supported in part by Government of Extremadura through project PCJ 100201 and GR10045. A. González-González is also grateful to the Ministry of Education, Culture and Sport for her FPU grant, reference AP2008-02546 and the support for a short stay in Évora (University of Évora, Cátedra BES Renewable Energies).

Bibliography

[1] Instituto Nacial de Estadística (INE), 2012. *Encuesta industrial de empresas 2011*. Madrid, España. (January 2013) (accessed 07.08.13.) Available online: `http://www.ine.es/prensa/np755.pdf`.

[2] González-González, A., Cuadros, F., 2013. *Continuous biomethanization of agrifood industry waste: a case of study in Spain*. Process. Biochem. 48, 920-925.

[3] APHA, AWWA, WPCF, 1992. *Métodos Normalizados para el Análisis de Aguas Potables y Residuales*, seventeenth ed. Díaz de Santos S.A., Madrid.

[4] Beltrán, J., Torregrosa, J., González, T., Domínguez, J.R., 2004. *Análisis Químico de Aguas residuales*, first ed. Abecedario, Universidad de Extremadura (I.C.E.).

[5] Proyecto ALTERCEXA, 2010. *Informe complementario sobre el estudio de soluciones viables para le aprovechamiento del biogás en Extremadura*, p.10 (January 2013) (accessed 07.08.2013.). Available online: `http://www.altercexa.eu/test/images/archivos/Areas%20Tematicas/Biogas/Estudio%20BIOGAS.pdf`.

[6] Ñaskeo Environment, May 2012. *Economy of Biogas Installations* (accessed 07.08.2013.). Available online: `http://www.biogas-renewable-energy.info/biogas_installations_investments.html`.

[7] EVE (Ente Vasco de la Energía), 2001. *Tecnologías avanzadas de generación eléctrica*. Energías renovables. Plantas de valorización de biogás de vertedero, p. 4.

[8] Abreu, E., April 2012. Estudio comparativo de la pared y cavidad torácica. Universidad Nacional Experimental "Francisco de Miranda", Venezuela (accessed 07.08.13.). Available online: `http://biblioteca.unefm.edu.ve/Anatomia%20Comparada%20de%20los%20Animales%20Domesticos/PARED%20Y%20CAVIDAD%20TORACICA-COMPARADA.pdf`.

[9] MITYC (Ministerio de Industria, Energía y Turismo), 2013. *Precio de los hidrocarburos* (January 2013) (accessed 07.08.2013). Available online: `http://geoportal.mityc.es/hidrocarburos/eess/`.

[10] Rodríguez-Abalde, A., Fernández, B., Palatsi, J., Flotats, X., 2010. *Efecto de los pretratamientos térmicos en el potencial de producción de metano de residuos cárnicos*. In: II Jornadas de la Red Española de Compostaje, Burgos (España).

[11] López Vázquez, R., Casp Vanaclocha, A., 2004. *Tecnología de mataderos*. Ediciones Mundi-Prensa, Madrid.

[12] Scharmer, K., Greif, J., 2000. *The European Solar Radiation Atlas*. In: Fundamentals and Maps, vol. 1. Les Presses del École des Mines, Paris.

[13] IDAE (Instituto para la Diversificacíon y Ahorro de la Energía). 2009. *Instalaciones de Energía Solar Térmica*, p. 100 (January 2013) (accessed 07.08.2013.). Available at: `http://www.idae.es/index.php/mod.documentos/mem.descarga?file=/documentos_5654_ST_Pliego_de_Condiciones_Tecnicas_Baja_Temperatura_09_082ee24a.pdf`.

Chapter 4

Construction, programming and operation of two state-of-the-art Vanadium Redox Flow and Lithium-ion batteries

4.1 Project PVCROPS

As previously referred, the work performed regarding the use of batteries to mitigate PV power fluctuations was the topic of FP7 project PVCROPS, short for "Photo-Voltaic Cost r€duction, Reliability, Operational performance, Prediction and Simulation" (Grant agreement no.308468). This project was formed by a consortium of twelve partners: European companies, universities, and the Moroccan government. The project began in November 2012 and lasted for three years (36 months) with a total budget of 5.4M€. The key objectives of this project were to improve performance, reliability and lifetime of PV systems, reduce costs of PV systems and mitigate power fluctuations to better integrate PV power in electrical grids. In the topic of reliability and integration of PV in the grid, the tasks set for the project can be divided into two major topics (work packages): one related with passive techniques to mitigate power fluctuations and the other by using active elements, (such as batteries, inverters, and EMS developed with specific objectives). The participation of UEVORA was focused on the latter, specifically in testing several different EMS (each with its own objectives) and better understand the characteristics and behaviour of batteries in these situations.

A project partner, UPNA, developed and simulated several EMS focused for PV systems (BIPV and PV plants) with a battery, each EMS with its own objectives: maximize the auto-consumption of PV power, stabilize the power exchanged with the grid, reduce power fluctuations in PV plants, among others. For the simulations, two new battery technologies were considered: Lithium ion and Vanadium Redox Flow batteries. The Lithium-ion battery technology was chosen due to its large adoption and maturity, and the promising Vanadium Redox Flow battery which has

had major important developments and has many advantages in some key areas, that make it interesting to study in more detail.

Lithium-ion technology has seen large improvements and is the first choice for many applications, such as cellphones and electric cars. It has as main advantages: large power and capacity densities, relatively high DOD (compared with lead-acid batteries), stable power delivery across a large SOC range, it is an abundant element and non-toxic. This technology disadvantages are: highly flammable, power and capacity are coupled which does not permit to tailor those parameters independently, and requires close monitoring and control of the voltage of each cell as an over-discharge can permanently damage the battery and an over-charge can make them explode. Moreover, the many materials used in lithium batteries are non-recyclable, its cost, although dropping, is still high, specially compared with other technologies used for similar cases (such as thermal storage in a CSP plant).

Vanadium Redox flow battery technology is one of the most recent but highly promising regarding large-scale stationary technologies. This technology has its name due to the electrolyte (in this case Vanadium) being dissolved in a liquid (sulphuric acid) which flows from a tank to an active area, where reduction/oxidation reactions occur during the charge/discharge of the battery. Main advantages of these batteries are: independence between power and capacity, scalability, long lifetime, increased safety (no risk of explosion), high depth-of-discharge (DOD), high round-trip efficiency, and components plus electrolyte are less hazardous to the environment than other batteries. All these features make these batteries ideal for almost any situation, although the relatively high control and pumps consumption make it more suited for very large applications (large power plants or large buildings/districts). A more complete description of this technology is provided in the next chapter.

Being relatively recent on the market, previous studies done regarding VRFB have been almost exclusively done by using models and simulations. These studies are useful to test different configurations, sizes, and other parameters, but they might overlook or disregard some operational or practical constraints that affect their performance and the validity of the simulations. These systems are typically very complex and a small change in one parameter might affect disproportionately the results. With this in mind, PVCROPS project was designed from the beginning to have two components: one where researchers developed EMS and batteries models to test and optimize their parameters, and another where those models and simulations were compared with experimental results of those same EMS tested in the two demonstrators. In this way, the models initially developed could be improved and refined to better match reality, providing a useful and more precise tool for future simulations of systems of this kind.

To this effect, UEVORA assembled two prototype systems to act as demonstrators, with real-size equipment to provide experimental data and test the integration of all components of these systems. Each prototype system was composed of:

- a new state-of-the-art battery (VRFB and LIB)
- a PV system (BIPV and ground PV plant)
- a building to provide loads
- connection to the public electrical grid
- a control system to operate the prototype system

Figures 4.1 and 4.2 show the schematic view of the VRFB and LIB prototype systems, respectively.

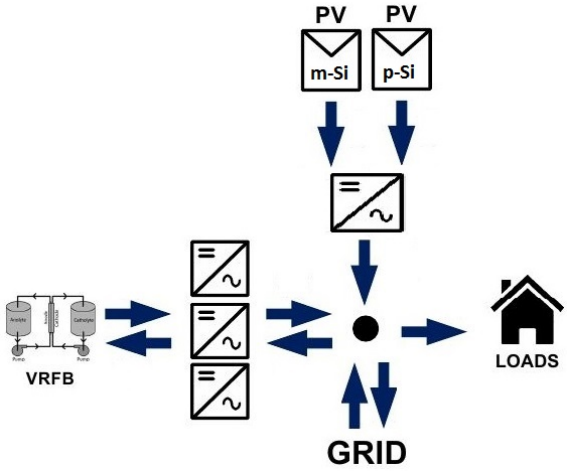

Figure 4.1: Schematic view of the VRFB prototype system with its main components: VRFB, 3-battery inverters, BIPV system(monocrystalline and polycrystalline strings), 2-MPPT PV inverter, loads, and grid.

The main tasks and objectives defined for the construction and operation of these prototype systems were to study and test several practical aspects of these kind of installations, namely: test and solve compatibility issues between different pieces of equipment from different manufacturers, test the efficacy of EMS to fulfill their objectives, test these new batteries in real conditions and their suitability for future applications, develop new software and hardware control systems, and obtain experimental data necessary for the proper modulation of the batteries. Unfortunately, the problems that occurred and some technical constraints that were found hindered the capacity to fulfill all of the initial objectives defined as targets for the project and for this and other theses.

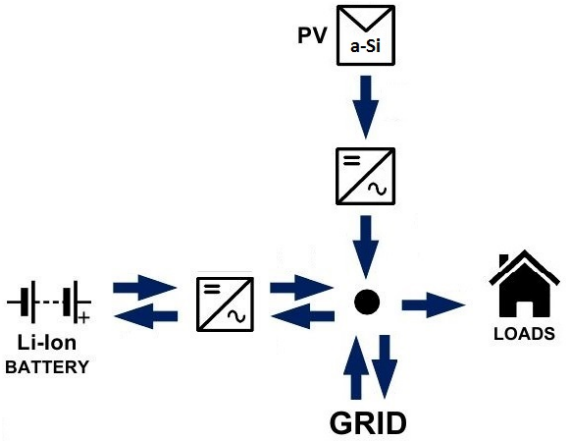

Figure 4.2: Schematic view of the LIB prototype system with its main components: LIB, battery inverter, PV plant (amorphous Silicon), PV inverter, loads, and grid.

4.2 Construction, programming and initial operation of the prototype systems

All different pieces of equipment (batteries, inverters, and PV plants), control systems and electrical circuits did not previously exist in UEVORA, so an initial work to prepare both sites (one for each battery technology) was necessary to be done, before the actual construction of the prototype systems. The entire construction, programming and operation of both prototype systems (VRFB) were part of two PhD thesis. This thesis focuses on the construction of both prototype facilities, software programming, and initial operation of the prototype systems. The other thesis will describe in more detail the instrumentation developed for various applications, and modeling of all different prototype components.

The construction, programming and operation of the two prototype systems was divided into the following stages:

1. Design of the prototype systems
2. Integration and compatibility of power equipment
3. Design, programming and test of the central control system
4. Construction of the VRFB prototype system
5. Construction of the LIB prototype system
6. Initial tests to determine operational parameters

4.2.1 Design of the prototype systems

To test the batteries in real conditions and be able to test different EMS, the prototype systems would have to fulfill several requirements. Two separate prototype systems were to be built, each with a battery and a PV system connected to a building, that in turn would be connected to the electrical grid. These systems would be controlled by some system that would have to allow the implementation of different EMS (each with its unique requirements). Taking into account the objectives of the project, requirements of EU commission, and budget limitations, the first equipment defined were the batteries. The VRFB would be provided by redT ([11]) , with a capacity of 60kWh and 5kW of nominal power, while the LIB would be bought by UEVORA with a capacity of 32kWh and 5kW of nominal power. After the batteries were defined, the size of each PV system was estimated, with the aid of simulations, to be, respectively, approximately 7kWp and 4kWp. As both PV systems and batteries produce/store electric power in DC, it would be necessary to convert the power from DC to AC, using power inverters to that effect.

All power inverters (battery and PV) were provided by Ingeteam. Those inverters would have to operate within the voltages and power ranges of each battery and PV system and be able to communicate with the batteries. An issue was found at this stage, as the VRFB operated with a maximum voltage of 65V while the battery inverters to be installed had their ideal voltage much higher (around 250V) and had a minimum DC voltage limit of 45V. Due to this limits, the inverter would operate with less efficiency, and the battery was limited to a maximum discharge voltage of 45V, which resulted in the loss of approximately 1% of useful SOC (capacity that can actually be used for charge/discharge). For the operation of the VRFB in this demonstrator, the voltage range was limited to 48V and 62V, as a safety margin.

To allow for the test of unbalanced loads in different AC phases, the VRFB was connected to the three-phase electrical grid, by three synchronized power inverters (one for each phase), while the LIB prototype was installed in a mono-phase grid. All electrical circuits had to comply with the Portuguese code and regulations regarding the power levels from both PV system, battery and loads. To be able to transmit and receive data, all power pieces of equipment required an Internet connection (via Ethernet), so a switch with multiple Ethernet ports was installed.

In UEVORA campus at Herdade da Mitra, Évora, Portugal, there was a PV plant of 10kWp that was not operating at the time due to faulty inverters, and for the PVCROPS project it would be necessary to communicate and operate wih inverters from Ingeteam. Since the PV panels were free to be used for other applications, it was decided to use them within PVCROPS. The PV plant was composed of three strings,

each of a different PV technology: monocrystalline, polycrystalline and amorphous Silicon. Coincidently, the amorphous string had a power rating of 3.3kWp while the other two technologies summed 6.74kWp of total power, approximately matching the PV plant sizes previously defined. The monocrystalline and polycrystalline PV modules were moved to the roof near the VRFB prototype site, while the amorphous modules were moved just outside the LIB prototype site. These work tasks where done by the UEVORA researchers, except for the roof panel installation done by a professional company. Figures 4.3 and 4.4 show both PV installations: 6.74kWp BIPV system in the roof, close to the VRFB prototype system site and the 3.3kWp PV system at the location chosen for the LIB prototype system.

Figure 4.3: Photograph of the BIPV system, mounted in the rooftop near the VRFB prototype site

Figure 4.4: Photograph of the PV plant, mounted in the ground near the LIB prototype site (right container behind the PV plant).

4.2.2 Integration and compatibility of batteries and inverters

Due to different voltage operating ranges of the batteries, PV systems and inverters, and as the manufacturers involved had not work together in the past, several issues occurred regarding the inter-compatibility of power equipment (mostly communications and voltage ranges).

Regarding the PV string within the LIB prototype system, no problems were found between PV string and the PV inverter, as the PV plant had a voltage and current limits within the specifications ranges of the inverter provided. The VRFB prototype PV system, as it was comprised of two strings of different technologies, the chosen PV inverter should ideally have two MPPT to maximize production for both strings and it should have a three-phase AC connection. Ingeteam had such an inverter in construction but it would take several months to be ready so it was decided to install two 1-MPPT mono-phase output inverters, while the other 2-MPPT and three-phase output inverter was not produced and available to be installed.

Due to safety and operational reasons, battery inverters need to receive some parameters (SOC, current, power, etc.) from the battery. As inverters and battery were made by different companies, each with different communication protocols, both pieces of equipment had to be adapted to allow a proper interconnection and proper functioning when connected together. There was an effort by all manufacturers (inverters, VRFB manufacturer and LIB manufacturer) to make changes in software to make both inverters and battery compatible but this process took several months with constant testing and debugging of problems only detected on site and during certain operating conditions

4.2.3 Design and programming of the central control system

Another necessity that arose while setting up the system was to allow the control system to communicate with the battery inverters, VRFB, and remaining instrumentation, and to run and test the necessary EMS. The chosen equipment was a PC with an in-house software (freely available online at `https://www.dropbox.com/sh/eadyhu2zpgujd8s/AAAsRdTCskost8ajaKeUIeHra?dl=0`) made in Labview to communicate with each equipment, log all data, and allow remote access and (limited) control of the whole installation. Figure 4.5 shows the front-end of the in-house developed control system software.

As each equipment had its own communication protocol and requirements, and as some EMS require a minimum of 1 second for each cycle run, a substantial effort followed to code and program the software to fulfill all these requirements. Figure 4.6 shows a schematic with the instrumentation and equipment that communicated with the central control system and their respective network communication interface. To be able to run any EMS, several functions were created to accommodate all necessary communication protocols: Modbus over TCP/IP with each inverter (to receive data and send commands), serial port to read an Arduino board with Python (to obtain

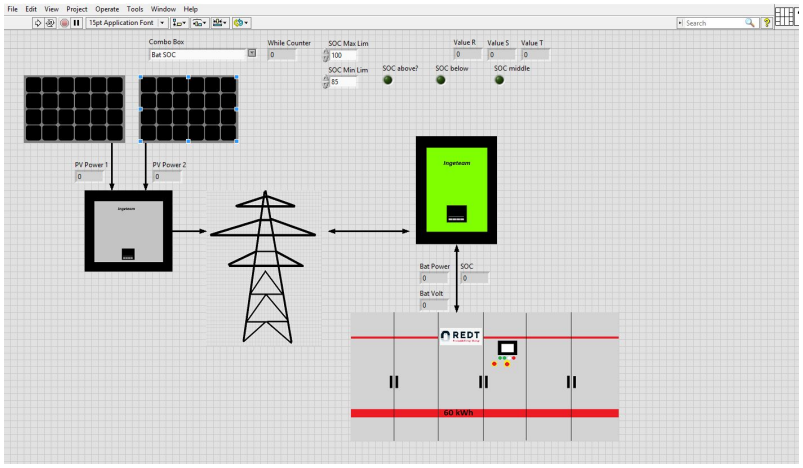

Figure 4.5: Screenshot of the developed Labview control system.

BIPV related data: radiation and cell temperature), Modbus RTU with wattmeters (to obtain the power exchanged with the grid and independent measures of power exchanged with the battery), VISA to read a Keithley multimeter (to measure the reference cell voltage and then compute the respective SOC), and finally to save data to a .xls or .csv file for posterior analysis. All these functions were used to implement EMS by receiving data and transmitting commands to all equipment to make them perform according to the EMS algorithm being tested.

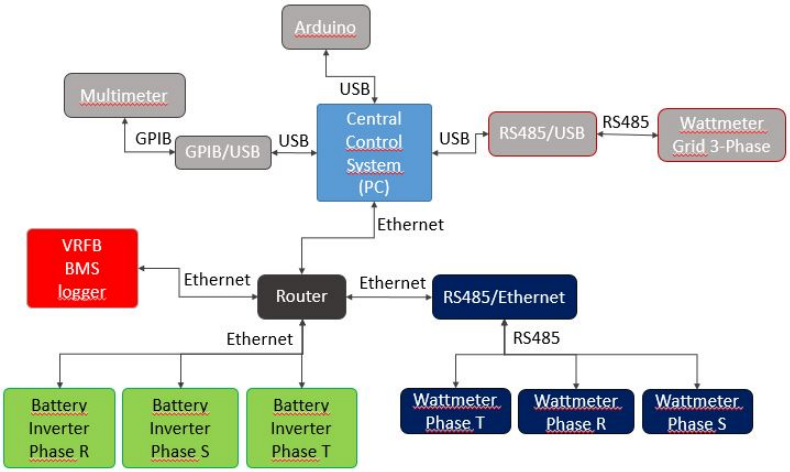

Figure 4.6: Schematic representation of the instrumentation used in the prototype systems and their respective network communication interface.

4.2.4 Construction of the VRFB prototype system

The VRFB demonstrator site had to provide appropriate conditions to accommodate every piece of equipment, allow the connection to the building and its electrical grid,

favorable location for the BIPV system, and controlled temperature. The chosen location was a building in Herdade da Mitra campus, within a porch facing North (ideal to minimize high temperatures during Summer months), with a roof nearby with sufficient area to install the BIPV system, connection to the Internet and electric system of the building. The porch was converted to a closed room to isolate and protect its interior, where most of the equipment was installed. The entire electric circuit was also installed to connect each component to the others and to the building, among other necessary facilities including AC unit, PC to act as a central control and data-logger, and Ethernet switch to provide Internet access to all pieces of equipment.

Figure 4.7: Photograph of the porch chosen for the VRFB prototype system, already with walls and doors. This site was designed to have ground access and allowed for easy assembly of the VRFB access for the required machinery.

Prior to the arrival of the battery, some special features had to be implemented. Due to the chemicals used in this battery technology, the electrolyte is formed by Vanadium dissolved in sulphuric acid, which in a case of a leakage could damage the building and/or harm people. A container bund was thus built and coated with an acid-resistant paint to secure the premises and to be able to hold the entire electrolyte in case of the worst-case scenario for a leakage: major breach of both tanks and complete failure of the battery safety measures. Along the electrolyte container, an emergency shower was also installed, as required by Portuguese laws regarding installations with corrosive materials. Figures 4.7 and 4.8 show the porch before and after the prototype system was installed.

As RFB technology allows electrolyte to be stored in tanks and for a complete electrolyte discharge, the transport of the battery from the manufacturer (located in the United Kingdom) to the demonstrator site (in Évora, south of Portugal) was done by shipping it completely disassembled. The assembly at the site required lifting machinery and several people working for two weeks to finish the installation. After pumping 3200 litres of electrolyte into the tanks, several tests were done to assure

Figure 4.8: Photograph of the site after the prototype system installation: PV and battery power inverters fixed on the wall(in the middle), acid-resistant coated bund (red area in the floor), and the VRFB (inside metal cabinet).

that the battery had no leakages, to verify its performance and operation during the initial charge and discharge cycles, and to verify if all sensors and electronic equipment were functioning as expected. During the initial tests, one PLC was damaged and took several days for a replacement to arrive.

This phase took several months until the prototype system was fully operational and all problems solved: faulty electrical components that had to be found and replaced, inverters presenting problems with their firmware (both PV and battery) and problems in the synchronization of the three battery inverters, electrolyte leaks, outside Internet access blocked (resolved through a requirement to gain permission made to the UEVORA IT department). Power peaks caused the circuit breakers to open (turning the AC power supply off) requiring their replacement and the installation of an UPS to assure the power supply and to filter those voltage fluctuations, among other situations.

Figure 4.9 shows a schematic of the VRFB technology and Figures 4.10 and 4.11 show interior photos of the installed VFRB.

To avoid a repetition of the description of the VRFB prototype system, the complete description of the demonstrator with technical data about each piece of equipment and detail of the EMS tested is provided in Chapter 5.

4.2.5 Construction of the LIB prototype system

The LIB prototype had similar constraints as the VRFB prototype system, although as this technology is more compact, it did not require such a large room. Of the available facilities, the site chosen was a container typically used in construction sites, located at Renewable Energies Chair PECS platform. This container had electrical

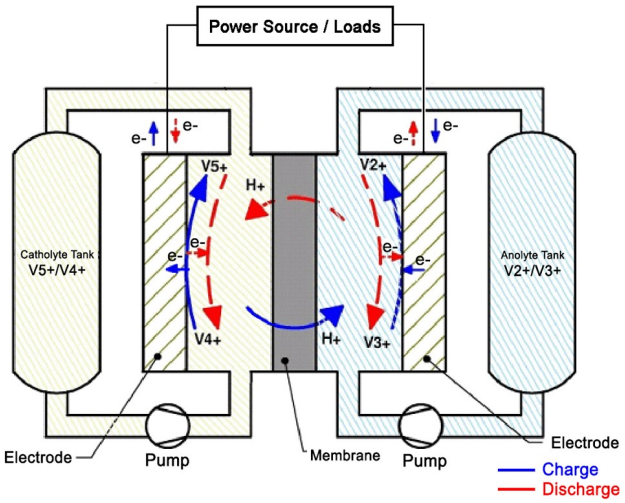

Figure 4.9: Schematic representation of the VRFB. Electrolyte is stored in two tanks (a catholyte tank, with positive charged Vanadium ions, and the other with "negative" (less positive) Vanadium ions. Two pumps force the electrolytes to flow to the stack where the redox reaction occurs and charges/discharges the Vanadium species.

and Internet connections, a nearby network to provide load, and a large area near the container where the PV system could be installed.

The minimum and maximum (air) temperatures in this place range from -5°C during Winter to 45°C during Summer, but inside the container, the maximum temperature could go above 50°C. The LIB has a temperature range of 15°C to 35°C so it was necessary to lower the temperature inside the container, as the battery and other equipment produce heat when functioning, contributing to the internal temperature control difficulties. A sun-blind and AC unit were installed to maintain the temperature within the acceptable range. Due to a problem in the internal ventilation system of the LIB, it was also necessary to add extra fans to force the air to pass through the lithium cells, and cool the battery. Figure 4.12 show the container with the LIB prototype system installed: LIB in the right (metal cabinet with blue drawers), control system (PC and multimeters in the desk at right) and PV and battery inverters (grey and green equipment in the back, behind the CPU tower).

The lithium-ion battery, a first from the manufacturer and specifically designed for this project, was scheduled to be installed at the same time as the VRFB demonstrator, but, unfortunately, due to several bureaucratic delays, the battery only arrived almost a year later. Adding to this delay, during the installation and operation of the Lithium-ion battery, several critical problems were found, which required the presence of technicians from the manufacturer to solve them. The tech-

Figure 4.10: Photograph of the positive tank (catholyte tank) of the prototype VRFB system. Each tank holds approximately 1800 liters of electrolyte. The pipes with larger diamenter (blue colour) transport the electrolyte throught the piping system while the translucid pipes provide the inert gas used to act as a "blanket".

nical visits took several months to happen and when all problems seemed to be solved, a new one would be found shortly after. These problems ranged from a sudden battery shut-down when someone walked inside the demonstrator room (later found to be because of a faulty relay), software bugs that would cause certain voltage values to swap and misread temperatures resulting in internal safety measures to be activated and battery shut down, faulty software and firmware that could only be solved by replacing a board, among other problems. Despite all efforts made, the battery remained with some software problems causing misreadings, making its safe operation impossible. For this reason, the remainder of this thesis will focus on the results of the VRFB as all tests based on the LIB prototype system could not be completed.

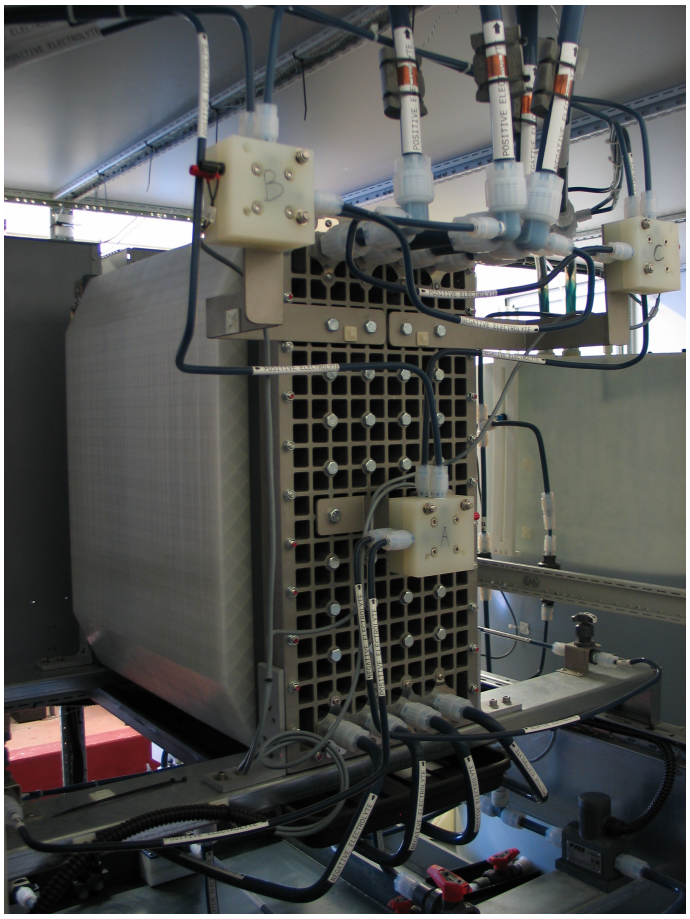

Figure 4.11: Photograph of the VRFB stack (rear view). This stack is composed of 40 series connected cells. Both electrolytes enter the stack from the bottom and leave on top. The two smaller square cells marked A, B, and C are three reference cells that measure the voltage of the positive and negative electrolyte at the entrance and the voltage of the positive electrolyte at the exit of the stack. These values are unchanged by the battery operation, and can then be converted to the SOC of the VRFB at any state and operation conditions.

4.2.6 Initial tests to determine operational parameters

After the construction and assembly of the VRFB prototype system, it was necessary to run several initial tests to assess some technical parameters about the batteries, inverters and overall system. Although some specifications are provided by manufacturers, these parameters might only be valid under certain conditions and the operational limitations that the VRFB was submitted to, could have a negative influence in those values. To this effect, several tests were performed to experimentally measure certain important parameters and to characterize the prototype system as a whole.

Figure 4.12: Photograph of the LIB prototype system. The battery has a total 32kWh (5.3kWh per blue drawer), and 5kW nominal power.

VRFB full charge and discharge cycle

The first test performed on the VRFB was a full charge and discharge cycle. This procedure allowed to obtain several important parameters and information such as: total capacity, battery (DC) efficiency, inverter conversion efficiency, SOC versus battery voltage, and response times, as well as test communications, data logging and the functioning of the diverse internal battery sensors. The SOC versus battery voltage curve is more detailed in the next Chapter.

Figures 4.13 and 4.14 show the voltage and current variations during full charge and discharge, respectively. From these graphics it is possible to observe how the inverter performs the charge or discharge of the battery. For a given power, the inverters apply a voltage below (if discharging) or above (if charging) the battery voltage, that is kept approximately constant until the current decreases the set power value. To compensate for the lower current, the inverters further decrease or increase the voltage in order to maintain the same power. This process occurs until the voltage reaches its operational limits, when after that the inverters cannot continue to discharge/charge at the same power, so it must decrease proportionally to the current decrease.

The active power being charged or discharged is given by Equation 4.1:

$$P_{DC}(t) = V_{DC}(t) * I_{DC}(t) \tag{4.1}$$

Using Equation 4.1, it is possible to plot the evolution of charge and discharge powers along the charging and discharging processes. Figures 4.15 and 4.16 show the DC power being charged and discharged, respectively. As one can see in the

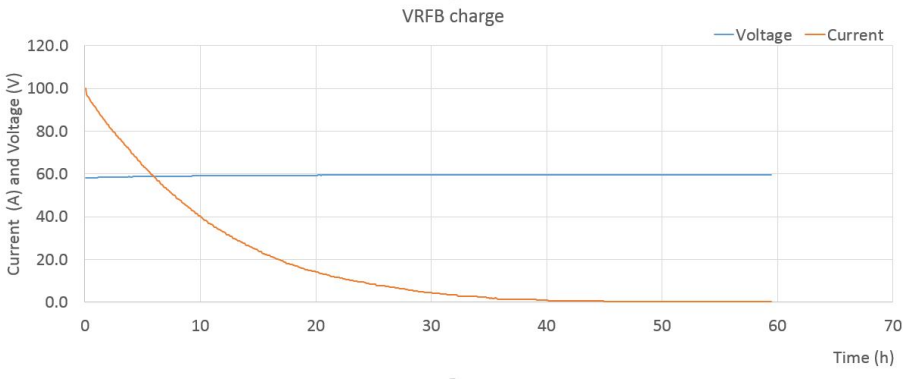

Figure 4.13: Variation of the voltage and current during the VRFB charge.

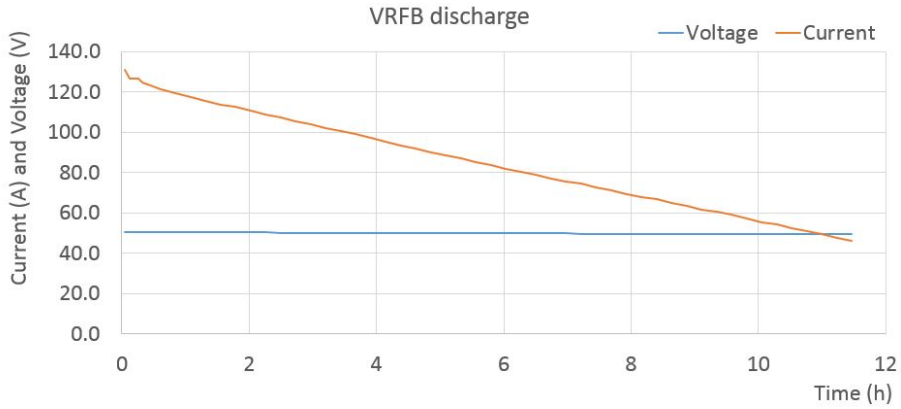

Figure 4.14: Variation of the voltage and current during the VRFB discharge.

graphics, the power being charged or discharged varies along the entire charging and discharging processes.

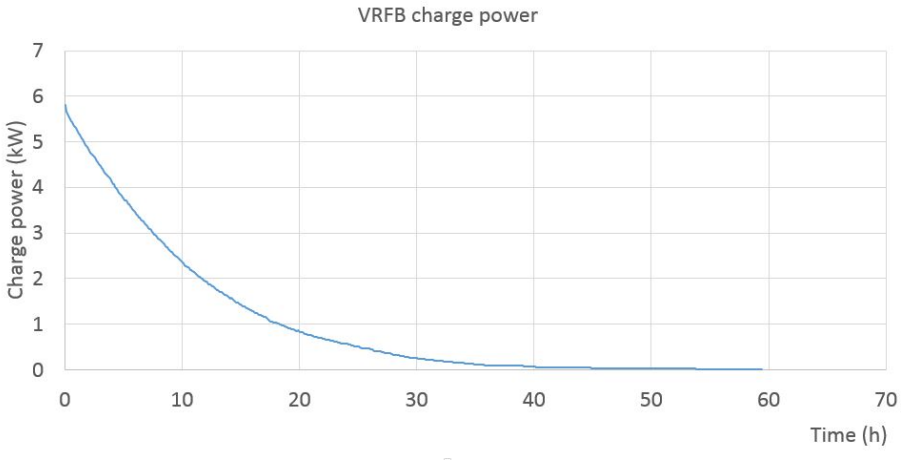

Figure 4.15: Variation of the charge power during the VRFB charge.

By plotting the power variation as a function of SOC instead of time (Figure 4.17) one can obtain an important curve, useful for EMS development as one must

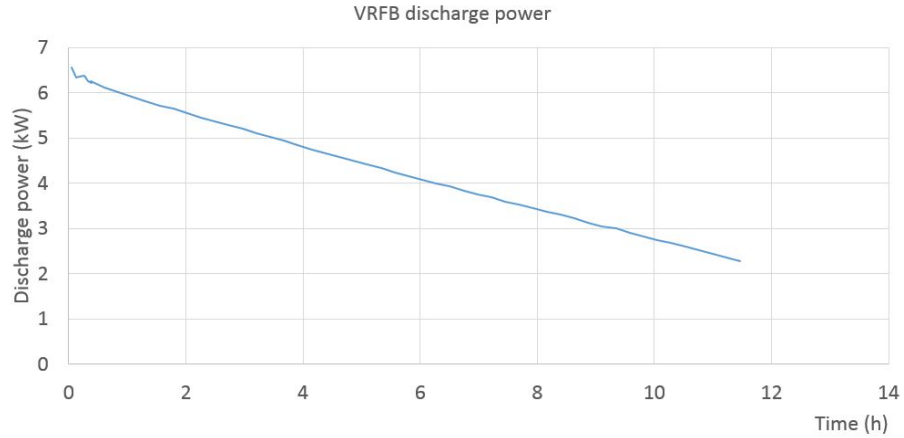

Figure 4.16: Variation of the charge power during the VRFB discharge.

take into account that the available power is not constant and has a large variation within the operational SOC.

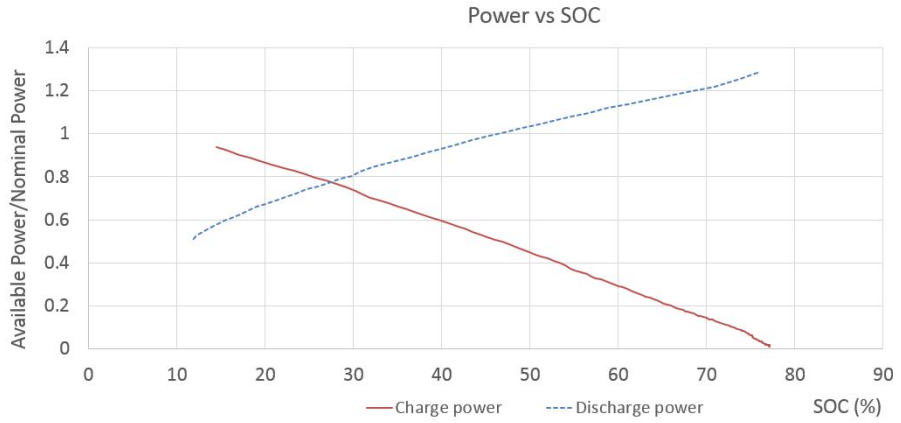

Figure 4.17: Variation of the charge and discharge available power as a function of the VRFB SOC.

The total capacity of the battery is given by Equation 4.2:

$$Capacity_{VRFB} = \int P_{DC\,charge}(t) \tag{4.2}$$

where $P_{DC\,charge}(t)$ is the power measured on the DC side that is being charged at each moment. By dividing the total discharged energy (computed by formula 4.2 but integrating the power charged) by the charged energy, one obtains the full cycle battery efficiency (η_{VRFB}), as shown in Equation 4.3:

$$\eta_{VRFB} = \frac{\int P_{DC\,discharge}(t)}{\int P_{DC\,charge}(t)} \tag{4.3}$$

The values obtained for the VRFB capacity and efficiency were 60.4kWh and 81.1%, respectively. These values match the one provided in the VRFB specifications: total capacity of 60kWh and a DC-DC round-trip efficiency between 70% and 80%, respectively. The results showed a difference of 0.7% and 1.4% (relatively to the upper range value), positive in both cases. The experimentally measured higher efficiency might come from the fact that the battery was discharged only to the 45V, whilst the value computed by the company can take the whole voltage range into account. As the discharge power significantly drops for lower SOC values, the conversion efficiency at those conditions decreases.

The battery efficiency should take into account the energy consumed by auxiliary equipment (such as pumps, BMS, logger, etc.) however those values were not taken into account as this battery is still in a prototype phase, the auxiliary equipment is over-sized for the dimension of this battery. Moreover, as the auxiliary equipment supply is done in AC, no energy stored in the battery is consumed.

VRFB inverters: DC-AC conversion efficiency

The VRFB charge and discharge are performed by the power inverters that are controlled by the control system. These inverters have a rated efficiency (conversion from AC to DC or DC to AC) of 94%. As however, this value is only achieved in ideal conditions, which are not met in this prototype system as the VRFB maximum voltage is only 65V, on the lower operating range of the inverter, this should affect the conversion efficiency. An experimental measurement of this parameter was performed to obtain the inverter AC-DC conversion efficiency value dependent on real operating conditions found in the VRFB prototype system. Using the charge and discharge data, one can obtain the inverter AC-DC (charge) conversion efficiency ($\eta_{inv\,AC-DC}$) using Equation 4.4:

$$\eta_{inv\,AC-DC} = \frac{\int P_{DC\,charge(t)}}{\int P_{AC\,charge(t)}} \tag{4.4}$$

where $P_{AC\,charge}(t)$ is the power measured in the AC side, while $P_{DC\,charge}(t)$ is measured on the DC side. In a similar manner, the inverter DC-AC (discharge) conversion efficiency ($\eta_{inv\,DC-AC}$) is given by Equation 4.5:

$$\eta_{inv\,DC-AC} = \frac{\int P_{AC\,discharge}(t)}{\int P_{DC\,discharge}(t)} \tag{4.5}$$

Using these equations, the measured AC-DC (charge) and DC-AC (discharge) inverter efficiencies were 91% and 85%, respectively. As one can see, the efficiency

changes while charging or discharging and these values fall short 3% and 9%, respectively, from the 94% of maximum efficiency provided in the specifications.

The whole energy storage system efficiency (η_{ESS}) can then be computed with Equation 4.6:

$$\eta_{ESS} = \eta_{inv\,AC-DC} * \eta_{VRFB} * \eta_{inv\,DC-AC} \tag{4.6}$$

For the VRFB prototype system, the value obtained was 62.7%. A system composed of a Lithium-ion battery with a DC-DC round-trip efficiency of 90% and with an operating voltage range closer to the ideal one for the inverter, would have a value of approximately 79%, representing a difference of 26% more than the value obtained for the VRFB prototype system.

Variation of efficiency with operational parameters

By using the full cycle data and by integrating the power along the whole charge and discharge processes, some effects are not being taken into account, namely the efficiency variation with power (voltage and current), and temperature. For example, when discharged, the battery has a voltage value of 45V and when charging, the inverter raises its voltage to make the current flow into the battery. As the inverter is more efficient at higher voltages, it is expected that the charge efficiency should be higher than when discharging. Moreover, for a given voltage, the efficiency also varies with the set current, which should also affect the efficiency.

This detailed study was scheduled to be done in the first months following the complete assembly of the VRFB prototype system but the issues found took several months to correct and left no time to do these studies (that although useful, were not essential), as other essential tasks were necessary to be done. A new schedule was made in which these tests would be performed after the run of all EMS, but, unfortunately, at the end of the project, a severe leakage of inert gas used to isolate the electrolyte tanks occurred, causing the electrolyte to react with air. This reaction severely affected the battery capacity and power. Until the electrolyte was restored, a process that took several months to design and put in practice, the VRFB was limited to approximately one forth of the capacity (15kWh), and a maximum charge/discharge power of 2.4kW. These parameters are far from the original ones, so a study of the variation of efficiency would yield values that could not be properly transposed and compared to the same VRFB operating in ideal conditions.

Measures are being taken to recuperate proper operation conditions, but the corresponding work will be taken over by other Ph.D. theses. Nevertheless proper

initial operation was possible as explained and research and development work was done resulting in the study of several EMS, as reflected in the next chapter and papers published.

Bibliography

[1] Renewable Energies Dynamics Technology Ltd.; PVCROPS case study, Available online: `http://www.redtenergy.com/case-studies/energy-storage-80kwh` (accessed on 28^{th} July 2016)

[2] Pascual, J., Sanchis, P., Marroyo, L., *Implementation and control of a residential electrothermal microgrid based on renewable energies, a hybrid storage system and demand side management*, 2014, Energies 7, pp. 210–237

[3] Ingeteam, Available online: `http://www.ingeteam.com` (accessed on 28^{th} July 2016

Chapter 5

Implementation and validation of a Self-Consumption Maximization energy management strategy in a Vanadium Redox Flow BIPV demonstrator*

Abstract

This paper presents the results of the implementation of a self-consumption maximization strategy tested in a real-scale Vanadium Redox Flow Battery (VRFB) (5 kW, 60 kWh) and Building Integrated Photovoltaics (BIPV) demonstrator (6.74 kWp). The tested energy management strategy aims to maximize the consumption of energy generated by a BIPV system through the usage of a battery. Whenever possible, the residual load is either stored in the battery to be used later or is supplied by the energy stored previously. The strategy was tested over seven days in a real-scale VRF battery to assess the validity of this battery to implement BIPV-focused energy management strategies. The results show that it was possible to obtain a self-consumption ratio of 100.0%, and that 75.6% of the energy consumed was provided by PV power. The VRFB was able to perform the strategy, although it was noticed that the available power (either to charge or discharge) varied with the state of charge.

Keywords: Vanadium Redox Flow Battery, BIPV, Energy Management Strategy, self-consumption maximization, real-scale battery

---

Luis Fialho[1,2], Tomás Fartaria[1,2], Luis Narvarte[3], Manuel Collares Pereira[1,2], Implementation and validation of a Self-Consumption Maximization energy management strategy in a Vanadium Redox Flow BIPV demonstrato, Energies 2016, 9, 496, doi:10.3390/en9070496

[1]Renewable Energies Chair, Universidade de Évora, 7002-554 Évora, Portugal (lafialho@uevora.pt, tomasfartaria@uevora.pt, collarespereira@uevora.pt)

[2]Universidade de Évora Instituto de Investigação e Formação Avançada (IIFA), Palácio do Vimioso, Largo Marquês de Marialva, Apart. 94, 7002 - 554 Évora, Portugal

[3]Instituto de Energía Solar, Universidad Politécnica de Madrid, 28040 Madrid, Spain (navarte@ies-def.upm.es)

5.1 Introduction

With the current increase of distributed renewable energies generators (such as rooftop photovoltaic power) in electrical grids, and more affordable energy storage systems (ESS), it is becoming much more viable to match individual demand for electricity with on-site PV production [1, 2, 3]. In the case of residential installations, the use of ESS for short-term management of supply, i.e., allowing the shift of PV energy to higher consumption periods (such as the evening peak or at night), could increase self-consumed electricity from 30% to 70% [4, 5, 6].

To allow this increase, a battery must be integrated in the grid-connected PV system and an *ad-hoc* energy management strategy (EMS) must be implemented in a control unit that correctly manages the electricity flow between the PV generator, the battery, and the grid. In recent years, several EMSs focused on the maximization of the self-consumption of on-site-produced PV electricity have been presented [7, 8, 9, 10], in which they assert that this strategy is useful and economically viable, even without feed-in-tariffs.

This EMS requires a reliable and efficient battery technology with low power/energy ratio, such as the Vanadium Redox Flow Batteries (VRFB). This promising technology has as main advantages the decoupling of power and capacity, a very long lifetime (reported as above 10000 cycles, or 25 years of operation), very low maintenance and deep discharge capability (almost 100.0%) [11]. Very few batteries of this kind exist in laboratories, specially in such a scale that allows real-life test conditions, so the investigation of this batteries is mostly done with simulations (and sometimes in small lab battery cells) [12, 13].

In order to test the performance of this kind of EMS, a real-scale VRB demonstrator was built in the University of Évora, part of the FP7 PVCROPS European project [14]. This demonstrator consists of a PV generator of 6.74 kWp, a PV inverter of 10 kW, a battery inverter of 7.4kW and a VRFB of 60 kWh. The main objective of this paper is to present the results of the validation tests of the self-consumption energy management strategy mentioned above and to show its suitability for building integrated PV applications. Useful conclusions for the future operation of this kind of systems are also discussed.

5.2 Real-scale VRFB demonstrator

The methodology used in this paper is based on the implementation of a real-scale demonstrator, installed at the University of Évora (Portugal). It consists of a rooftop

mounted PV system (BIPV), an electrical storage system (Vanadium Redox Flow battery), both connected to a building, which in turn is connected to the public electric grid (see Figure 5.1).

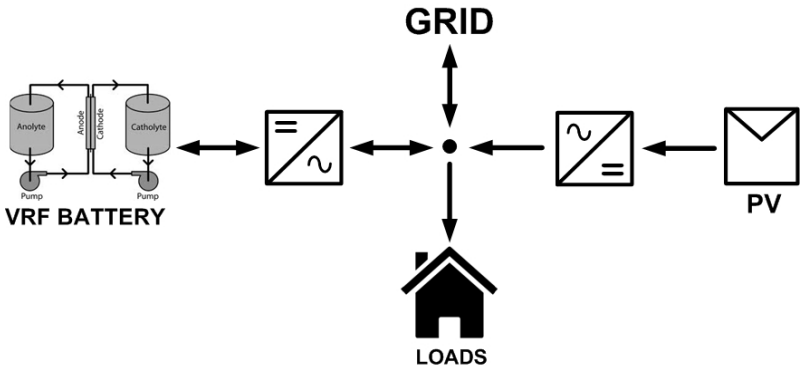

Figure 5.1: Demonstrator (photovoltaic (PV) plant and Vanadium Redox Flow battery (VRFB) with respective converters) simplified schematic. Inverters convert power from PV and battery (DC) to the grid (AC).

5.2.1 Equipment

The BIPV system is composed of two strings, a 3.24kWp of monocrystalline PV panels and 3.5kWp of polycrystalline cells, connected to a three-phase power inverter [15] with two independent maximum power point tracking (MPPT), connected to the building AC power grid. The energy storage is provided by a Vanadium Redox Flow Battery with 5kW nominal power and 12h storage [11], providing a total capacity of 60kWh. The battery is also connected to the triphasic AC grid by three synchronized inverters (one per phase) [15]. Figure 5.2 shows the rooftop mounted PV system while Figure 5.3 shows the battery and four inverters (PV inverter in gray and the three battery inverters in green).

To operate the demonstrator, a control system was implemented using a PC with Labview software to send and receive commands, and for overall system communication. This PC also acts as data logger to receive and store data. This PC receives data with parameter values from all the equipment (inverters, battery, and other sensors), runs the Labview software with the EMS, and continuously ensures the operation safety. In addition, each equipment has its own safety measures and surveillance implemented.

The main innovative feature of this demonstrator is the usage of a real-scale Vanadium Redox Flow Battery. Table 5.1 shows the main technical specifications

Figure 5.2: Roof mounted PV system

Figure 5.3: VRFB (right) and the inverters (left)

of the VRFB installed in the demonstrator. Table 5.2 shows the three battery inverters specifications, and Table 5.3 shows the photovoltaic inverter manufacturer specifications.

In this battery, the electrolyte is stored in two tanks (for positive and negative species). The electrolyte is then pumped through the piping system to a stack of cells where the reduction–oxidation reaction occurs. The electron exchange takes place in cells (connected in series to constitute the stack) where a special ion membrane separates the two electrolytes and only permits H^+ and V^+ to pass.

The use of two tanks and a stack allows the decoupling of the battery power density (determined by the active area of the cells in the stack) from its energy density—i.e., the total energy that it can store (given by tank capacity and specific electrolyte energy density). This energy–power decoupling allows a battery to be

tailored for many special cases, such as low power and large capacity (residential BIPV) or large power and lower capacity to mitigate power fluctuations (wind farms or PV plants). Another important feature of this battery technology is the absence of self-discharge, as there is no reaction outside the stack.

Table 5.1: VRFB technical specifications.

Specifications	**Value**
Manufacturer	REDT
Capacity	60 kWh (5 kW for 12 h)
Rated Power	5 kW
Maximum Operating Voltage	62 V
Minimum Operating Voltage	48 V
Electrical connection	Three-phase
Lifetime	+10,000 deep charge/discharge cycles
Full cycle (discharge/charge) Energy Efficiency	70%–80%

Table 5.2: Battery inverters technical specifications

Specifications	**Value**
Manufacturer	Ingeteam
Model	EMS Home 2.4
DC Max Current	50 A
DC Operating Voltage Range	48 V–250 V
Rated AC Power	2.4 kW
Electrical connection	single-phase

Table 5.3: PV inverter technical specifications

Specifications	**Value**
Manufacturer	Ingeteam
Model	3Play 12.5TL M
PV Power Range	12.9 kW–16.8 kW
DC Voltage Range MPPT1 and MPPT2	200 V–820 V
Rated Output AC Power	12.5 kW
Electrical connection	three-phase

Another distinct characteristic of this battery is the usage of vanadium as the main electrolyte element. The VRFB exploits the ability of vanadium to exist in four different oxidation states: from V^{2+} through V^{5+}, dissolved in sulfuric acid (H_2SO_4). It is used as the positive electrolyte (V^{5+}/V^{4+}) and as the negative electrolyte (V^{2+}/V^{3+}). The usage of only one element allows the restoration of the electrolyte by simply mixing both electrolytes (positive and negative) and then separating them again by recharging the battery. This process (electrochemical

reversibility) makes the electrolyte virtually infinite and non-degradable. The only source of electrolyte degradation is the occurrence of a side reaction with elements in air. To avoid this unwanted reaction, the empty space in the electrolyte tanks is filled with a high purity inert gas (Argon).

As these batteries are mostly composed of plastic piping and tanks and as the electrolyte is isolated from air, its lifetime is longer than other technologies, reported as 10,000 cycles [11]). In addition, as previously referred to in the introduction, another important feature of this technology is that it allows very deep discharges (close to 100%), so the whole battery capacity can be used.

Determination of the State of Charge

The VRF battery installed in this demonstrator is equipped with a parallel electrolyte circuit that carries a small part of the electrolyte flow to just one external cell (called reference cell) that is neither subjected to charge nor discharge. As this cell voltage is only affected by the real electrolyte state, this cell voltage is the actual battery voltage in a rested state (not influenced by charge or discharge). Also, the state of charge (SOC) is proportional to this voltage, so by knowing the reference cell voltage, one can obtain the real SOC.

The function relating SOC with reference cell voltage was obtained experimentally by the battery manufacturer. Figure 5.4 shows the SOC variation with the battery voltage (determined by the reference cell voltage multiplied by 40, as the stack is formed by 40 cells in series). In order to obtain the SOC value during the battery operation, this graphic was fit to Equation 5.1 so the SOC is computed using the reference cell voltage measurement. Equation 5.1 was defined as a piecewise function, computed as a numerical fit of the data within the operating ranges (from 41.8V to 65.4V), as no single function could properly be fitted. Each function was chosen as the one that yielded the best numerical fit for their respective ranges (R-Squared $\geqslant 0.99$).

$$SOC(V) = \begin{cases} 0.0031V^4 - 0.5606V^3 + 37.848V^2 - 1136.7V + 12810, & \text{if } 41.8\text{V } ¡ \text{ V} \leqslant 52.4\text{V} \\ -0.1544V^3 + 25.961V^2 - 1443.4V + 26577, & \text{if } 52.4\text{V } ¡ \text{ V} \leqslant 58.8\text{V} \\ 0.0609V^3 - 11.88V^2 + 773.28V - 16694, & \text{if } 58.8\text{V } ¡ \text{ V} \leqslant 65.4\text{V} \end{cases} \tag{5.1}$$

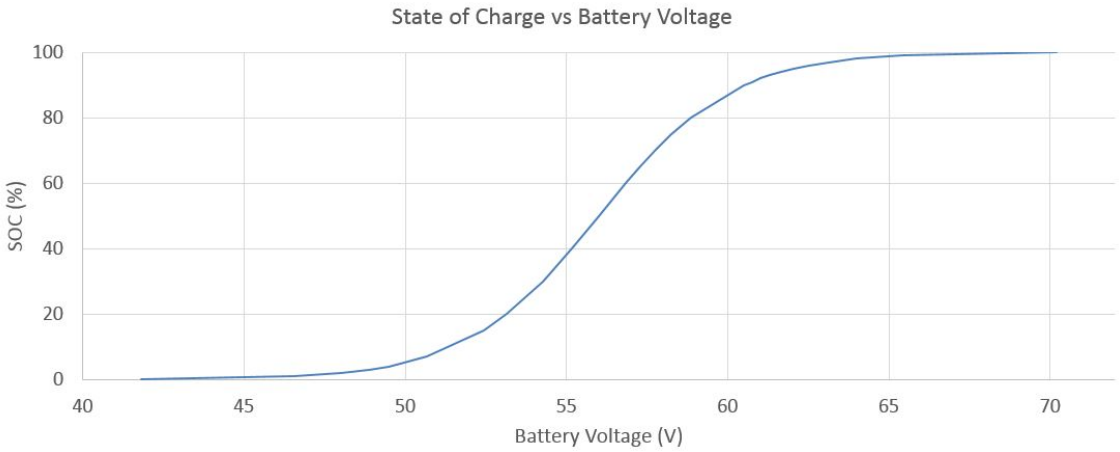

Figure 5.4: State of charge versus battery voltage. The battery voltage is determined by the voltage of the reference cell multiplied by 40 as the stack is formed by 40 cells in series.

5.2.2 Instrumentation and data acquisition

In order to properly implement an EMS, several parameters are measured allowing the computation of useful variables that enable the smooth running of the system operation. Furthermore, to allow a more complete study of each equipment, several additional measurements (other than critical variables already provided by the equipment) are necessary. Table 5.4 summarizes the monitored variables. For example, regarding the PV system, it is only necessary to know the AC Power given by the inverter. However, to evaluate the efficiency of the PV system or detect problems, more data is necessary (global radiation in the plane of the BIPV system, PV cells temperature and wind speed). These measurements are made using a weather station on the roof constituted of a pyranometer, a temperature sensor and an anemometer, as showed in Figure 5.5. These sensors are read and processed by a control electronics (arduino Leonardo board), which in turn sends the data via a wireless zigbee network to another arduino connected to the main PC.

The logged variables regarding the battery and inverters system are: DC power, AC power, battery voltage, current and state of charge (SOC). Other useful variables are also read to ensure that the installation is healthy and operating within safe conditions (for example battery temperature, piping flow and pressure, electric grid parameters and safe battery voltage range). The data is transmitted with Modbus protocol over TCP, via Ethernet. In order to obtain a more precise SOC value, being a crucial parameter, an independent digital bench voltmeter was installed to the reference cell. This independent measurement allows a precision improvement from 0.7% (battery control measurement) to 0.1% (multimeter measurement) of the reference cell voltage. Furthermore, a three phase wattmeter (power analyzer) was

Figure 5.5: Pyranometer and anemometer installed on the roof.

installed to measure the power exchanged from the BIPV system and battery to the electric grid. Also, three wattmeters were installed to obtain AC power measurements for each phase/ battery inverter.

Table 5.4: Monitored variables during the demonstrator operation. BIPV: Building Integrated Photovoltaics.

BIPV	**PV inverter**	**Battery**	**Battery Inverter**	**Grid**
Global Radiation	AC Voltage	Ref. Cell Voltage	AC Voltage	AC 3-phase power
PV Cell temperature	AC Current	Temperature	AC Current	
DC Voltage	AC Power	DC Voltage	AC Power	
DC Current		DC Current		
DC Power		DC Power		

5.2.3 Electrical Loads

The loads used for the tests were simulated using the building to which the demonstrator is connected, as the consumption of all building loads is much larger than the power and capacity of the battery and PV system. The loads were simulated as being equally distributed by the three phase electric grid. In this way, whenever a load is to be supplied, the power is sent to the building grid and that same power value is subtracted from the wattmeter measurement. This operation yields the power that would be exchanged with the grid if the loads were real and directly connected to the demonstrator. The load profile used is based in real 15 minute interval measurements made during a year of a real domestic installation [16]. This profile was then scaled according to the demonstrator specifications, in order to provide a load pro-

file level balanced to the system scale in what concerns battery usage and installed PV power. This method allows the loads to be of a suitable size relative to the real system specifications.

5.3 Self-consumption maximization strategy

The strategy tested in the demonstrator was the self-consumption maximization strategy. The main objective of this EMS is to maximize the consumption of PV energy produced locally in the building, hence avoiding injecting energy to the electrical grid. This is achieved by giving priority to PV power and either storing the residual load (energy produced by PV system minus the energy consumed by loads) in an ESS or by taking energy stored previously. Thus, the only exceptional case in which there is an exchange of energy with the grid is when the battery can no longer absorb more energy or when the PV + battery system cannot provide enough energy to the required loads.

According to the regulation of certain countries (such as Spain, Germany, Portugal, South Africa, Puerto Rico, etc.), the feeding of PV power into the electrical grid is either forbidden or highly restricted, so it is necessary to take measures to avoid this situation [17] [18], [19], [20], [21]. Either the excess power should be curtailed, i.e., PV production is limited to a sub-optimal value to avoid producing more power than what is being consumed at the moment, or, ideally, the excess power would be either stored or used by some deferrable loads (for example, a water heater, washing machine, etc.) [16].

In countries where a feed-in tariff (FIT) is paid for renewable electrical energy, the use of a battery could help to maximize profit. It could ensure that no PV power is lost due to regulatory restrictions or technical problems (for example, a sudden power outage) and even delay the sale of energy to a time when it might be purchased at a higher value (such as during peak hours). In a stand-alone system or in one where no PV power is allowed to be sold to the electrical grid (or if the selling price is too low), the user can store the energy for later usage, lowering the necessity to buy electricity from the grid.

A flowchart of the self-consumption maximization strategy is presented in Figure 5.6. In the first step, the control system acquires data from PV production, loads consumption, and the battery state of charge (SOC). Then, it computes the difference between the loads consumption and PV production, referred to as residual load ($P_residual$). If the differential is positive, it means that current PV power is not enough to supply the loads. Hence, $P_residual$ is provided by the battery (if it

has enough accumulated energy). If the battery cannot provide the total necessary power (due to a low SOC), the remainder has to be provided by the electric grid. The reverse happens when there is more PV power being generated than consumed in a given moment. In this case, the remainder should be stored in the battery. If the battery cannot absorb all of the excess power (for instance, near maximum SOC), the remaining power must be fed to the grid (considering the case with no active loads management).

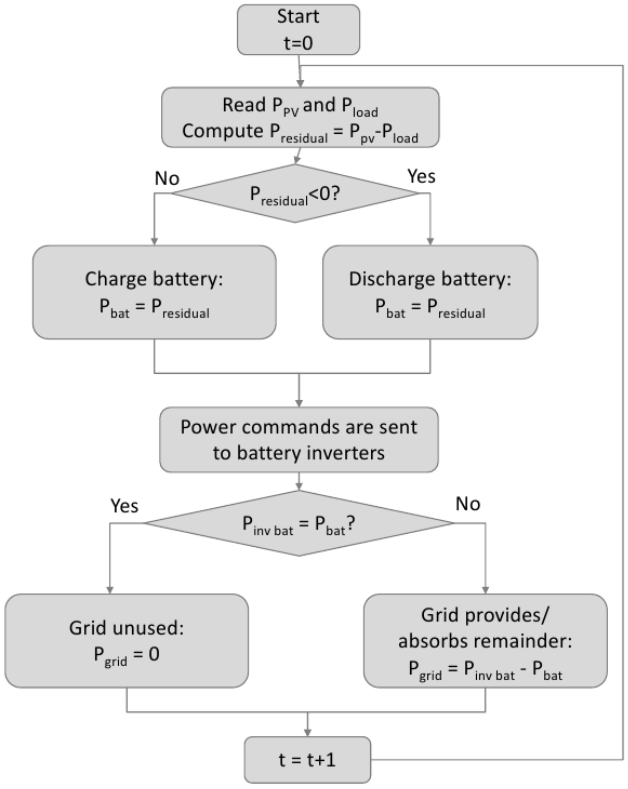

Figure 5.6: Flowchart of the self-consumption maximization strategy implemented in the demonstrator.

This cycle should run at least every second to provide a quick response to any changes in PV production, consumption, or other situations (for example a blackout or a sudden problem in a piece of equipment). In this way, the grid is not largely affected by large fluctuations in PV production that could otherwise be fed to the electric grid with poor quality (high power variations in a short time).

With the proper implementation of this EMS, the benefits obtained should be: lower energy exchange with the public grid, higher self-consumed PV power, and a higher load supply with PV power (either directly or by the battery). In order to validate this EMS—tested in the real size VRFB demonstrator—the following merit factors were defined to quantify the obtained improvements: self-consumption ratio, maximum positive (from the grid), and negative (into the grid) peak grid power,

respectively given by Equations 5.2 to 5.4).

$$\text{Self-consumption ratio} = \frac{\int_0^\infty (\mathrm{P}_{PV}(t) + \mathrm{P}_{grid}(t))\,\mathrm{d}t}{\int_0^\infty \mathrm{P}_{load}(t)\,\mathrm{d}t} \tag{5.2}$$

$$\text{Maximum positive } P_{grid} = Max\{\overline{P_{grid\,15min}}\} \tag{5.3}$$

$$\text{Maximum negative } P_{grid} = Min\{\overline{P_{grid\,15min}}\} \tag{5.4}$$

and $\overline{P_{grid\,15min}}$ is the average value for each 15 minute time interval, given by:

$$\overline{P_{grid\,15min}} = \frac{1}{900}\sum_{t=0}^{900} P_{grid}(t) \tag{5.5}$$

where t is time in seconds.

5.4 Validation of the self-consumption maximization strategy in the VRFB demonstrator

5.4.1 Testing campaign

A testing campaign was carried out in the time frame of one week. It was considered a sensible duration for the EMS validation, representing a balance between a short-time test (one day) and a longer period—for instance, one month. Figure 5.7 shows fifteen minute averages of the main parameters (PV power, loads consumption, and power exchanged with the battery) recorded during the testing of the Self-Consumption Maximization strategy. Figure 5.8 shows the power exchanged with the battery and the power exchanged with the grid in the same time period.

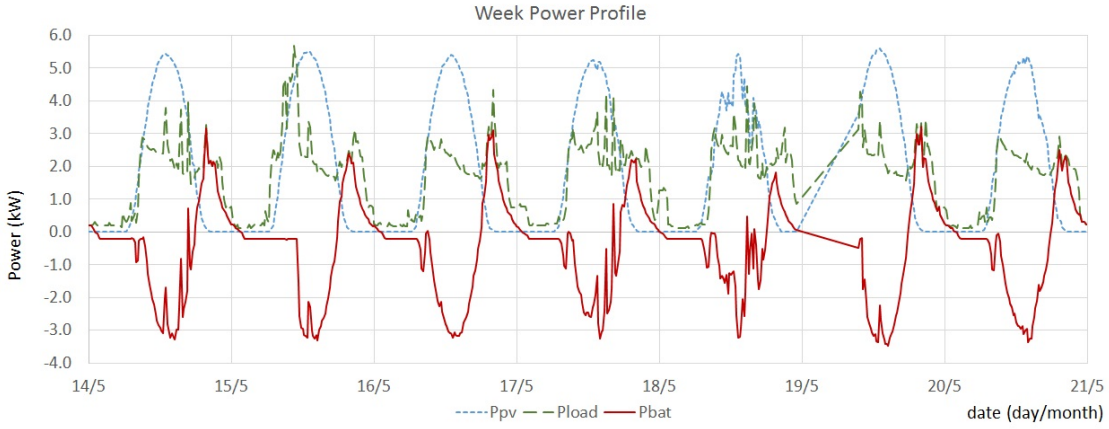

Figure 5.7: One week display of the PV, loads, and battery power profiles (P_PV, P_{load}, and P_{bat}, respectively).

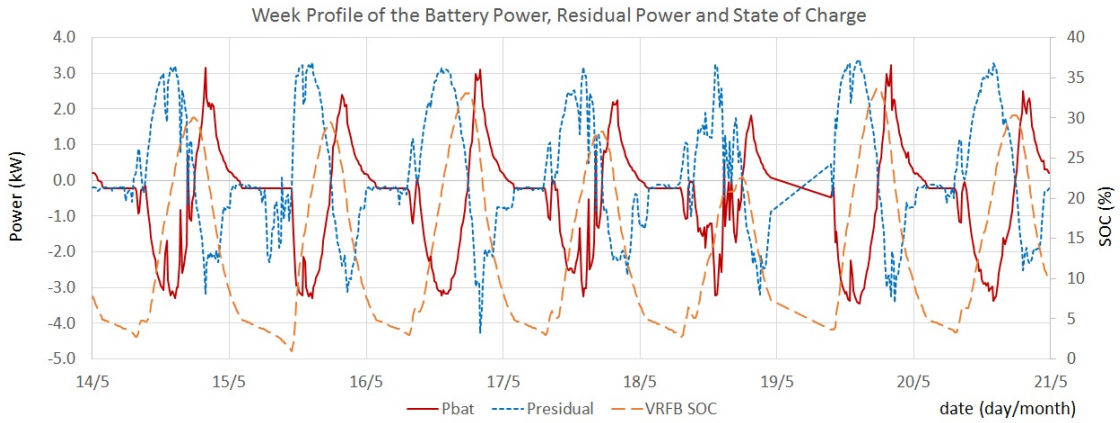

Figure 5.8: Variation of P_{bat}, $P_{residual}$, and state of charge (SOC), one week period.

Figure 5.9 shows the solar radiation on the PV plane (pyranometer) and PV cell temperature in the same time period.

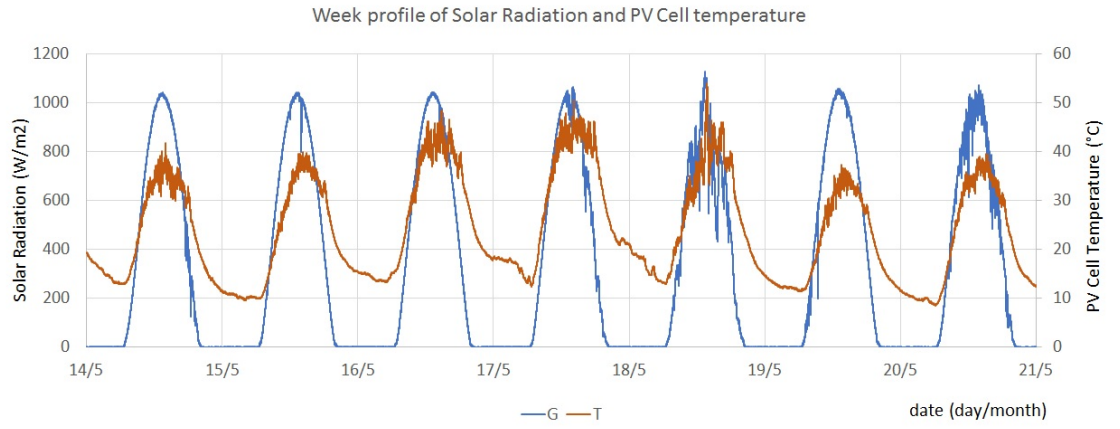

Figure 5.9: Week profile of Solar Radiation (PV plane) and PV Cell Temperature.

From the graphics shown in Figures 5.7 and 5.9, the PV generation (blue doted line in Figure 5.7) was mostly regular, with a clean radiation profile with only one day with significant variation (seen in Figure 5.9 at 18/05/2015). When the PV power is higher than the consumption, the remaining power (residual load positive) is stored in the battery (battery power is negative when charging). Usually, later in the day, when PV power is decreasing, the residual load (negative) is supplied by the battery.

However, when comparing Figure 5.7 with Figure 5.8, it can be seen that despite the energy stored in the battery being enough to supply the loads, the power that the battery can deliver was not enough. This is due to the ratio of power versus SOC not being constant throughout the major range of SOC. When the battery is partially discharged (lower SOC), the discharge power that it can provide is lower

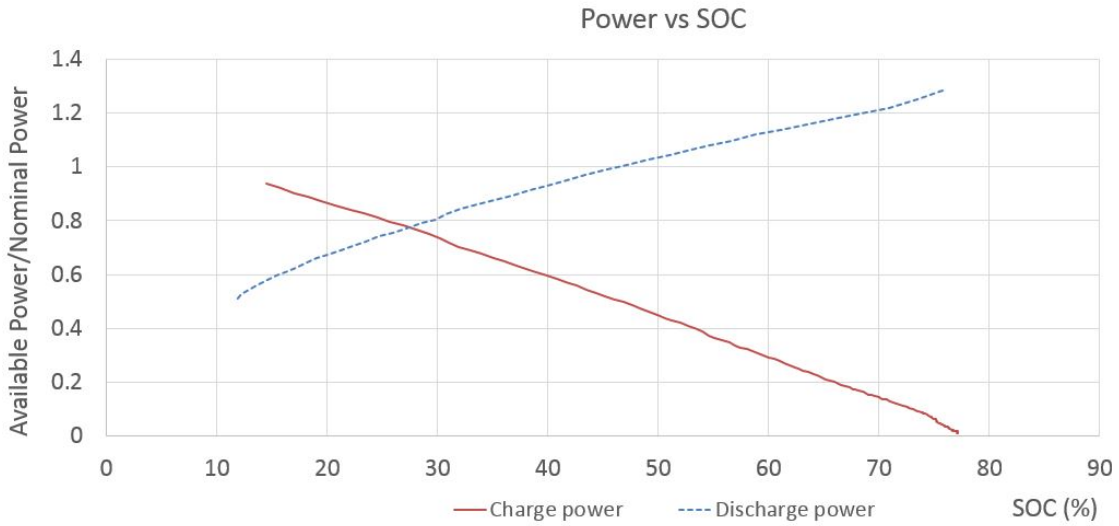

Figure 5.10: Variation of available discharge (blue) and charge (red) power relative to the nominal power with the battery SOC.

than the nominal power. The reverse situation occurs with the charge power when the battery is almost at full capacity (higher SOC), as shown in Figure 5.10.

Figures 5.11 and 5.12 show that, at the beginning, the residual load (blue line) began to be entirely supplied by the battery (red line). When the battery got below 5% of SOC (purple line), the loads had to be supplied by the grid, as below this value, the battery voltage gets close to the inverter minimum voltage range. To avoid this situation, a safety measure was implemented. In Figure 5.11, one can see that despite this safety measure, the battery SOC continued to fall suggesting that the value used to charge the battery is not enough to overcome the consumption of the inverters and the battery internal losses.

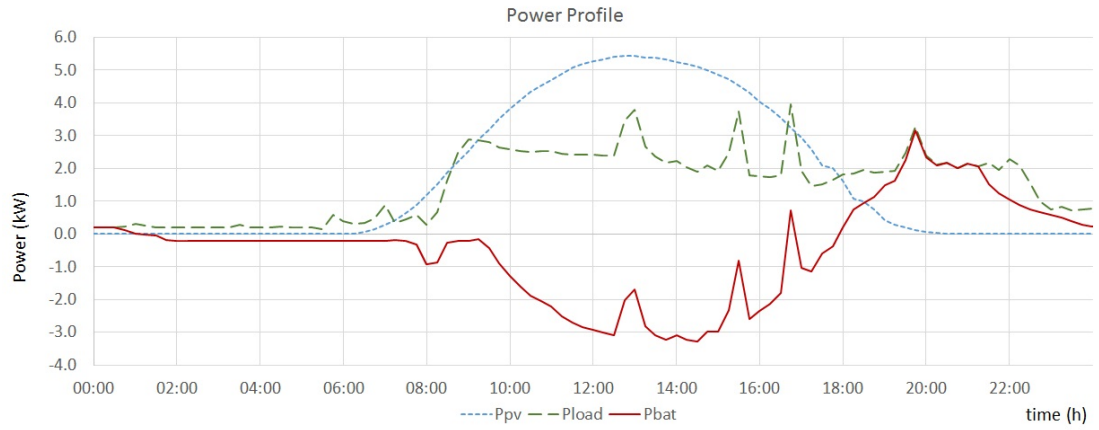

Figure 5.11: First day of the self-consumption maximization test.

When the PV power began to increase, the residual load also began to increase

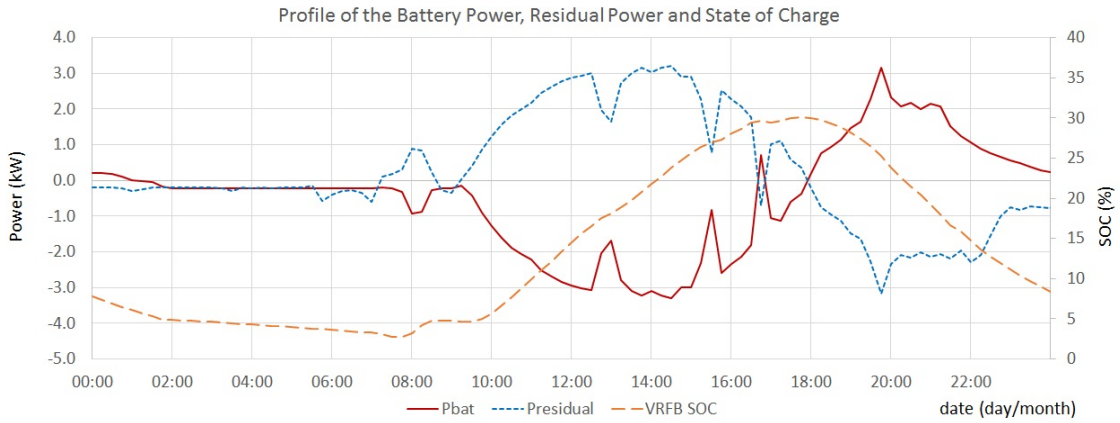

Figure 5.12: Display of the first day of the self-consumption Maximization test.

(positively), so the available power is used to charge the battery. At the end of the day, when PV power decreased, the previously stored energy is used to supply the loads. At the end of the day (after 21h) some power had to come from the grid as the battery could not provide entirely the necessary power to the evening load peak.

5.5 Results

To properly assess the validation and to quantify the self-consumption maximization performance, several merit factors were computed and compared with the case in which the demonstrator did not have an ESS.

Table 5.5 shows the comparison summary of the merit factors for the demonstrator with and without storage, evaluating the overall EMS performance for the testing period. Table 5.6 shows the merit factors computed for each day of the testing period.

In terms of total energy, the installation was able to self consume 100.0% of the PV generation and it was able to supply 75.6% of the total consumption, hence it was necessary to get 24.4% of the energy from the grid. The maximum peak power from the grid was 2.5 kW, without energy injection into the grid. Considering the demonstrator without storage, only 65.2% of the total energy generated by the PV system is self-consumed, and the peak power injected to the grid was 3.3 kW, while the peak power taken from the grid reached 4.2 kW.

To decrease the grid contribution, it is possible to increase the installed PV power or decrease the loads power consumption. In order to have a flexible demonstrator system, allowing the testing of different EMS that can require larger storage capacity, the total installed battery capacity ended up not being completely used in

this test.

This occurrence hints the opportunity to develop and implement strategies that can provide more benefits than an exclusively short-term or long-term EMS. The remaining unused battery capacity can be used as reserve power in case of a unforeseen blackout, to take advantage of electricity price fluctuations, to provide power to neighbor installations or even to charge electric vehicles. Also a higher available PV power could be stored in the battery for later use, decreasing the grid necessity. The extra capacity relative to the PV system size also raises the important question on how to optimize the battery capacity regarding the PV generation and loads consumption.

Table 5.5: Comparison between the full demonstrator and a virtual one without storage.

Merit Factor	**Storage**	**No Storage**
Self-consumption ratio (%)	100.0	65.2
Maximum positive peak P_{grid} (kW)	2.5	4.2
Maximum negative peak P_{grid} (kW)	0.0	3.3

Table 5.6: Comparison between demonstrator results with and without storage.

Date		**Self Consumption Ratio (%)**	**Maximum Positive Peak P_{grid}(kW)**	**Maximum Negative Peak P_{grid}(kW)**
14/05	storage	100.0	1.2	0.0
	no storage	67.5	3.2	3.2
15/05	storage	100.0	2.5	0.0
	no storage	61.6	3.1	3.3
16/05	storage	100.0	1.4	0.0
	no storage	63.5	4.3	3.2
17/05	storage	100.0	2.1	0.0
	no storage	66.1	2.6	3.2
18/05	storage	100.0	2.6	0.0
	no storage	66.4	3.2	3.2
19/05	storage	100.0	1.2	0.0
	no storage	65.5	3.4	3.4
20/05	storage	100.0	1.2	0.0
	no storage	66.9	2.5	3.3

This test yielded several useful results for the future operation of this technology demonstrators:

- The Vanadium Redox Flow technology has the ability to decouple power and capacity but the available power at extreme SOC varies. Figure 5.10 shows the

variation of discharge (blue) and charge (red) power with the SOC. This fact also reveals the importance of analyzing these systems as power sources/sinks and not only in terms of global energy.

- The system formed by the VFRB and inverters has achieved an overall average efficiency of 57.7% during the testing period. The efficiency is penalized by the battery operating voltage range being bellow the ideal voltage range of the inverters. The used inverters have a working voltage ranging from 48 V to 300 V, although their efficiency is higher at the top end of this range [15].
- The inverters consumption and battery internal losses are not entirely supplied during the safety procedure. Although the VRF battery is not damaged by an over-discharge, a voltage below the working range can turn the battery inverters off (the battery inverters are powered by the battery and require a minimum of 45 V), hence disturbing the normal operation of the installation.

5.6 Conclusions

The test results of the use of a VRFB as the storage system for the testing of a self-consumption maximization strategy, implemented in a real-size demonstrator, were presented. The results show that the VRFB is a suitable technology to be combined with BIPV systems.

Regarding the EMS testing, the strategy successfully maximized the consumption of locally-produced PV energy. Using the battery to store excess PV power (positive residual load), it was possible to completely avoid the injection of energy into the public electric grid—i.e., 100.0% self-consumption ratio. In addition, the total energy consumed by the loads was 75.6%, supplied by PV generation. A closer analysis of the system operation shows that an increase in PV power could further decrease the necessity of the electrical grid, as a large part of the battery capacity (approximately 65.0%) was unused.

The correct performance of the EMS is also shown by the reduction of power exchanged with the grid. The peak power from the grid was reduced in 59.0% in comparison with the case without energy storage. This means that the prosumer, apart from benefiting the whole electrical system, not only reduces their electric bill due to the reduction of grid energy consumption, but also due to the reduction of the utility contracted power tariff.

This work also showed the relevance of the equipment operational limits (in this case, the battery inverters DC voltage range) to the EMS, and the non-negligible

variation of available charge/discharge power with the battery SOC. In future developments of energy management strategies, all these operational limitations should be taken into account to ensure the proper and safe working mode of the whole system as planned.

5.7 Acknowledgments

The authors would like to acknowledge the support of this work, developed under the PVCROPS Project, which has received funding from the European Union's Seventh Framework Programme for research, technological development and demonstration under grant agreement $n°308408$. This work was also supported by the Renewable Energies Chair of the University of Évora (PhD scholarship, author Luis Fialho) and by a PhD scholarship (author Tomás Fartaria) from FCT – Fundação para a Ciência e Tecnologia, Portugal, Grant number SFRH/BD/84396/2012.

The authors also would like to acknowledge the support of the European Commission OPENAIRE FP7 Post-Grant Open Access Pilot for supporting the publication of this work.

Bibliography

[1] Richter, N., Is Rooftop Solar Finally Good Enough to Disrupt the Grid? 2015. Available online: https://hbr.org/2015/05/is-rooftop-solar-finally-good-enough-to-disrupt-the-grid (accessed on 11 April 2016)

[2] Feldman, D., Barbose, G., Margolis, R., James, T., Weaver, S., Darghouth, D., Fu, R., Davidson, C., Booth, S., Wiser, R., Photovoltaic System Pricing Trends: Historical, Recent, and Near-Term Projections. 2014. Available online: http://www.nrel.gov/docs/fy14osti/62558.pdf (accessed on 11 April 2016)

[3] International Energy Agency (IEA). Global EV outlook: Understanding the electric vehicle landscape to 2020. 2013. Available online: http://www.iea.org/publications/globalevoutlook_2013.pdf (accessed on 11 April 2016)

[4] Rickerson, W., Couture, T., Barbose, G.L., Jacobs, D., Parkinson, G., Chessin, E., Belden, A., Wilson, H., Barrett, H., Residential Prosumers-Drivers and Policy Options (Re-Prosumers). 2014. Available online: http://iea-retd.org/wp-content/uploads/2014/06/RE-PROSUMERS_IEA-RETD_2014.pdf (accessed on 11 April 2016)

[5] Solar Power Europe. Global Market Outlook, For Solar Power 2015–2019. Available online: http://www.solarpowereurope.org/insights/global-market-outlook/ (accessed on 11 April 2016)

[6] Vrettos, E., Witzig, A., Kurmann, R., Koch, S., Andersson, G., Maximizing local PV utilization using small-scale batteries and flexible thermal loads. 2013. Available online: http://www.eeh.ee.ethz.ch/uploads/tx_ethpublications/Vrettos_etal_2013.pdf (accessed on 11 April 2016)

[7] Zaheeruddin, Manas, M., Renewable energy management through microgrid central controller design: An approach to integrate solar, wind and biomass with battery. Energy Rep. 2015, 1, 156-163

[8] Merei, G., Moshövel, J., Magnor, D., Sauer, D.U., Optimization of self-consumption and techno-economic analysis of PV-battery systems in commercial applications. Appl. Energy 2016, 168, 171-178

[9] Lang, T., Ammann, D., Girod, B., Profitability in absence of subsidies: A techno-economic analysis of rooftop photovoltaic self-consumption in residential and commercial buildings. Renew. Energy. 2016, 87, 77-87

[10] Pascual, J., Barricarte, J., Sanchis, P., Marroyoa, L., Energy management strategy for a renewable-based residential microgrid with generation and demand forecasting. Appl. Energy. 2015, 158, 12-25

[11] Renewable Energies Dynamics Technology Ltd., PVCROPS case study. Available online: `http://www.redtenergy.com/case-studies/energy-storage-80kwh` (accessed on 11 April 2016)

[12] Sum, E., Rychcik, M., Skyllas-kazacos, M., Investigation of the V(V)/V(IV) system for use in the positive half-cell of a redox battery. J. Power Sources. 1985, 16, 85-95

[13] Rychcik, M., Skyllas-Kazacos, M., Characteristics of a new all-vanadium redox flow battery. J. Power Sources 1988, 22, 59-67

[14] PVCROPS. Available online: `http://www.pvcrops.eu` (accessed on 11 April 2016)

[15] Ingeteam. Available online: `http://www.ingeteam.com` (accessed on 11 April 2016)

[16] Pascual, J., Sanchis, P., Marroyo, L., Implementation and Control of a Residential Electrothermal Microgrid Based on Renewable Energies, a Hybrid Storage System and Demand Side Management. Energies. 2014, 7, 210-237

[17] Puerto Rico Electric Power Authority (PREPA), Minimum Technical Requirements for Photovoltaic Generation (PV) Projects. 2012. Available online: `http://www.nrel.gov/docs/fy14osti/57089.pdf` (accessed on 23 June 2016)

[18] Red Electrica de España, Instalaciones conectadas a la red de transporte: requisitos mínimos de diseño, equipamiento, funcionamiento y seguridad y puesta en servicio. 2005. Available online: `http://www.ree.es/sites/default/files/01_ACTIVIDADES/Documentos/ProcedimientosOperacion/PO_resol_11feb2005.pdf` (accessed on 23 June 2016)

[19] Republic of South Africa Grid Code Secretariat (NERSA), Grid connection code for renewable power plants (RPPs) connected to the electricity transmission system (TS) or the distribution system (DS) in South Africa. 2012. Available online:

http://www.nersa.org.za/Admin/Document/Editor/file/Electricity/TechnicalStandards/South%20African%20Grid%20Code%20Requirements%20for%20Renewable%20Power%20Plants%20-%20Vesion%202%206.pdf (accessed on 23 June 2016)

[20] Bundesverband der Energie (BDEW), Technical Guideline Generating Plants Connected to the Medium-Voltage Network: Guideline for generating plants connection to and parallel operation with the medium-voltage network. 2008. Available online: https://www.bdew.de/internet.nsf/id/A2A0475F2FAE8F44C12578300047C92F/$file/BDEW_RL_EA-am-MS-Netz_engl.pdf (accessed on 23 June 2016)

[21] Ministério do Ambiente, Ordenamento do Território e Energia, Governo de Portugal, Decreto Lei n. 153/2014. 2014. Available online: http://www.legislacao.org/primeira-serie/decreto-lei-no-153-2014-306472 (accessed on 23 June 2016)

Chapter 6

Conclusions and future work

6.1 Conclusions

This section provides a broad resume of the conclusion drawn from the work performed in this thesis. More specific conclusions were drawn in the end of each chapter and in the papers.

PV technology seems to have gained a momentum that will keep rising for many years to come. Current and expected future advancements make this technology ubiquitous for almost any kind of application and are a major contender for powering developing countries in lower latitudes, but not exclusively. Many studies are being done to make the transition from the traditional fossil fuel to renewable (particularly solar) smooth and without major problems.

The first part of this work was dedicated to develop a model to help estimate mutual-shading in PV plants. The first reasearch question demanded an answer that could be flexible, to allow multiple configurations and customizable parameters, and that could provide useful results for PV plant operators, owners, builders, etc. The model developed can be implemented in any ray tracing software and has the advantage of allowing a custom configuration of the PV modules (fixed or mounted in trackers), program back-tracking procedures and even test other tracking options, and the user as complete control over the assumptions and limitations of the simulation done, which is not the case of most programs available in the market. The case study used to test the model showed that the PV plant in question could have annual energy losses of 4%. The losses found are high enough to affect energy production projections and economic studies.

The second part of this thesis presents the study performed to evaluate the suitability of mixing two different energy sources togheter to obtain a cleaner and more stable power output. The case studied was the hybridization of a biogas power plant with a PV plant. The study began with the sizing of the biogas power plant

then added the PV plant. It was found that to better take advantage of the PV power profile and to take into account some cloudy or rainy days, a biogas storage facility would be added. This storage would be used to store the excess biogas that wasn't burned when there was enough PV power to sell and/or consume during the operation of the plant. The sensibility analysis showed that with the increase of PV power installed, better would be the expected return and the payback period would be shorter. Despite the extra costs with extra PV modules, larger biogas storage container. The IRR and PBP improved from 7% and 10 years, respectively, to 9 years and 9% with the increase of PV power installed from 205.25kWp to 225.25kWp.

The final part of this thesis answered to some of the practial questions regarding energy storage and production in practical systems. Can state-of-the-art technology be integrated and operate to perform the strategies developed to solve some PV power issues? To provide answers, some EMS were tested in a PV system with storage connected to the electrical grid, and connected or not to a building (with loads) and the suitability of advanced batteries to this effect. Despite the many challenges and problems found during the construction of the two studied demonstrators, several conclusions could be drawn. Regarding the VRFB, it was found that the available discharge and charge power varied significantly with the VRFB SOC. This effect is non-negligible when applying a given EMS as it can unexpectedly limit the power expected to be injected/taken from the battery. It was also found that the battery inverters that were used, were significantly penalized by the VRFB battery voltage operating range. In the worst case, the AC-DC conversion efficiency was reduced by 9%. The whole ESS efficiency, i.e., the measured AC-DC-AC roundtrip charge-discharge efficiency was 62.7%, a low value when compared with the efficiency of other technologies. Operational constraints penalized this value, mostly the battery inverters loss of efficiency due to operating at low voltages.

Despite the limitations found, the battery was able to perform as expected regarding the time of response, suitability of capacity and power to the PV system and general operating conditions. By realizing a charge (from a completely discharged state) and measuring the charging power, it was possible to plot the total energy in the battery (SOC) change with the voltage of the reference cell. As the reference cell is not perturbed by the charge/discharge, it is possible to obtain a true measure of the SOC at any time. This feature is one of the major advantages and differences between traditional electrochemical batteries (such as Lithium, acid-lead, etc.) and the flow batteries, that can then be used to operate the battery more safely and to develop preciser EMS. The results obtained also helped to validate and improve the

VRFB model used for simulations and development of future EMS.

From the battery functioning standpoint, it was found that the integration of the VRFB with more mature equipment is not trivial and that it must be done properly to easily integrate this battery into an existing facility. As the VRFB was still a prototype, many expected faults occurred and were found during its operation. Faults ranged from the leaks in both electrolyte and gas, faulty electrical components, faulty pumps, operating limits due to the inverters requirement of a DC voltage above 45V to operate, safety and space related limitations, among many other small issues that despite not being critical or extremely dangerous, can hinder the proper functioning of the whole installation. Fortunately, as the VRFB manufacturers were included as partners of PVCROPS project, there was a constant communication and close accompanying of the work done, which allowed solving expected and unexpected problems as quickly as possible. The construction and operation of this VRFB prototype allowed its manufacturer to detect and correct many issues, which now results in a commercial product that can be sold.

Regarding the Lithium-ion battery, no relevant tests could be done due to the many impediments so no conclusions were taken, apart from the large difficulties that the installation of this kind of systems has.

The experience of design, projection, construction, and operation of both demonstrators brought valuable information related to the behavior of the used equipment in real conditions. There are still many improvements to be made regarding every aspect of the system and the construction of new prototype systems and the continuous improvement of existing ones will play a major role in their future developments.

6.2 Future perspectives and lines of investigation

As it became evident throughout the description of the work done in this thesis, a lot more can be done regarding the hybridization of PV power with other power sources, and specially with experimental tests to validate the many models already developed but not completely validated.

In many regions, the access to electricity comes from a power generator fueled by diesel or some other pollutant fuels. Despite being able to provide continuous and stable power output, these generators consume fuel that must be imported, adding transportation costs and necessity to buy large quantities to maintain a certain stock. Moreover, the pollutants resultant from the fuel burning are harmful to the ambient and nearby people, and requires frequent maintenance, that if a certain

component needs to be replaced, might take weeks to arrive, and there might be nobody nearby who knows how to repair it. With the decrease of PV prices (and other renewable technologies), it began to be more profitable to add a small PV system as main power source and supplement it with the diesel generator (the fuel saved acts as energy storage) than to have the same generator running during the whole day. Other power sources can be complemented with PV power, and many pilot projects are appearing and being tested allover the world.

Regarding energy storage, and specifically the VRFB technology, many improvements are still necessary to make this technology more able to compete with more established ones. Only recently VRFB have been commercialized and many new improvements can still be done regarding its chemistry, piping system, stack, new materials, etc.. The manufacturer of the VRFB prototype wants to continue the battery operation, even after the PVCROPS project has finished. Several new procedures have been done, including the restoration of the electrolyte that due to a air leakage, reacted with the air and lost a large part of its capacity. Also new reference cells were installed to maintain the battery actual and running. This infrastructure, almost unique in the world, can be an important instrument for new studies and developments in this area.

Finally, many technical problems that had hindered the tests of more EMS are now solved (although the Lithium-ion battery remains inoperable) so more experiments can be performed. With the tendency for electrical grids to increase in complexity and with the advent of smart-buildings, smart grids, the "internet-of-things", and electric cars, many new configurations appear and the study of their management and power supply is mandatory to ensure their seamless integration with the current grid. Here is where new EMS will play a crucial role to minimize energy losses, increase efficiency and make batteries economically viable and profitable, instead of some current systems that had to install them for necessity. Cheaper PV and batteries, allied with proper EMS, can make traditional energy consumers become independent from utilities and the public electrical grid, or even transform them as power/energy producers that sell excess power to the grid.

Annex

Posters and papers

The Annex is comprised of 5 documents that were part of the work done during this thesis, that due to their specific form, were not suitable for the main text of this thesis.

The first three posters (Performance Characterization of a Vanadium Redox Flow Battery, Validation of a Energy Management Strategy for a BIPV System with a Vanadium Battery Demonstrator, Validation of a Energy Management Strategy for a BIPV System with a Lithium Ion Battery Demonstrator) were presented in the EUPVSEC 2015, European PV Solar Energy Conference and Exhibition, in Hamburg Germany.

The last poster Good and Bad Practices in PV Plants was presented in the 28^{th} European Photovoltaic Solar Energy Conference and Exhibition, in Paris, France, 2013, and was later published in the proceedings Good and Bad Practices in PV Plants.

All in-house developed software for the control and acquisition of data from all equipment and instrumentation is freely available online at `https://www.dropbox.com/sh/eadyhu2zpgujd8s/AAAsRdTCskost8ajaKeUIeHra?dl=0`.

Performance Characterization of a Vanadium Redox Flow Battery

Luis Fialho[1], Tomás Fartaria[1], Manuel Collares Pereira[1]
[1] ST Renewable Energies Chair, Universidade de Évora, Portugal

Vanadium Redox Flow Battery

Specification	Value
Number of cells	40
Tank volume	2x1800 l
Maximum current	200 A
Nominal Power	5 kW
Storage capacity	60 kWh
Battery inverters nominal power	3x2.4 kW

Test 1 – Full Cycle Charge/Discharge Efficiency cell

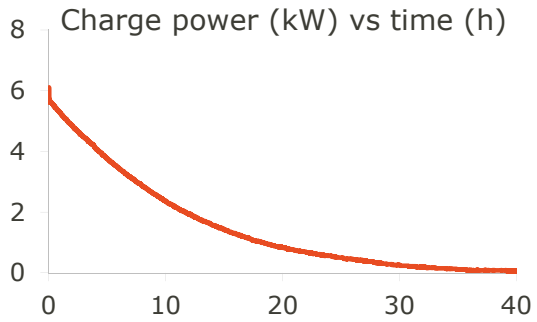

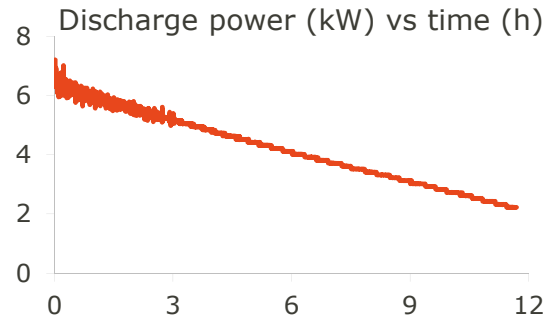

Test 2 – State of Charge (SOC) vs Voltage of reference

Conclusions:

The tests performed are in accordance with the specifications provided by the battery manufacturer.

The inverters voltage range limit the battery capacity to 60 kWh.

The reference cell voltage is not affected by the battery charge/discharge state. The reference cell allowed a precise SOC measurement.

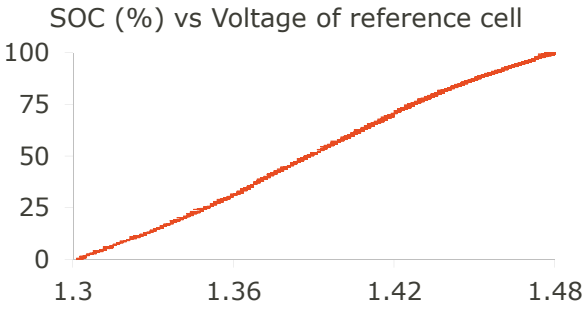

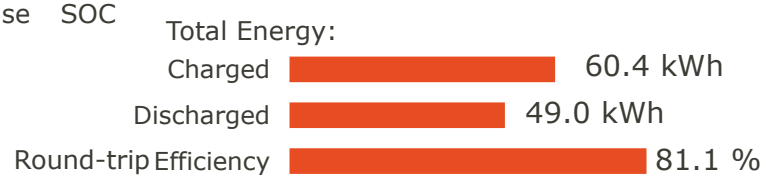

For more information see also poster "Validation of a Energy Management Strategy for a BIPV System with a Vanadium Battery Demonstrator".

PV CROPS
SEVENTH FRAMEWORK PROGRAMME
GOVERNO DE PORTUGAL
ST Renewable Energies Chair
UNIVERSIDADE DE ÉVORA
QUADRO DE REFERÊNCIA ESTRATÉGICO NACIONAL
POPH QUALIFICAR É CRESCER.
UNIÃO EUROPEIA Fundo Social Europeu

Validation of a Energy Management Strategy for a BIPV System with a Vanadium Battery Demonstrator

Luis Fialho[1], Tomás Fartaria[1], Manuel Collares Pereira[1]
[1] ST Renewable Energies Chair, Universidade de Évora, Portugal

BIPV System Demonstrator

Vanadium redox flow Battery:

- 5 kW nominal power
- 60 kWh capacity

Battery Inverters: 3x5 kW nominal power

PV installation: 6.6 kWp (m-Si and p-Si)

PV inverters: 3x2.7 kW nominal power

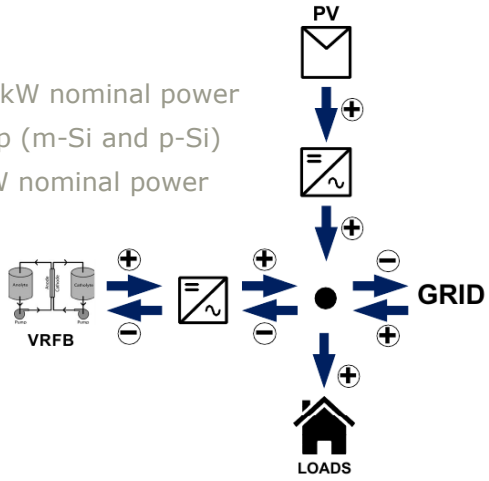

Self Consumption Optimization Strategy

Objective:
The main objective of this strategy is to maximize the consumption of locally produced PV power, hence minimizing the injection of power into the electrical grid.

Implementation:

$$P_{setBat} = P_{pv} - P_{load}$$

$$P_{grid} = P_{setBat} - P_{bat}$$

Due to battery operational limits (Voltage and SOC), a control to avoid overdischarge/charge was implemented.

P_{setBat}	AC Power command to battery inverter
P_{pv}	PV AC power
P_{load}	Loads AC power consumption
P_{grid}	AC Power exchange with the grid
P_{bat}	Measured battery inverter AC power

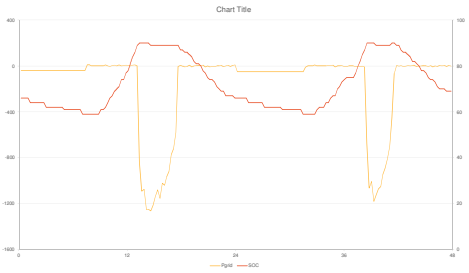

GOVERNO DE PORTUGAL
QUADRO DE REFERÊNCIA ESTRATÉGICO NACIONAL
ST Renewable Energies Chair
UNIVERSIDADE DE ÉVORA
PV CROPS
SEVENTH FRAMEWORK PROGRAMME
POPH QUALIFICAR É CRESCER.
UNIÃO EUROPEIA Fundo Social Europeu

Validation of a Energy Management Strategy for a BIPV System with a Lithium Ion Battery Demonstrator

Luis Fialho[1], Tomás Fartaria[1], Manuel Collares Pereira[1] , Aitor Makibar[2]
[1] ST Renewable Energies Chair, Universidade de Évora, Portugal
[2] Instituto de Energía Solar, Universidad Politécnica de Madrid, Spain

BIPV System Demonstrator

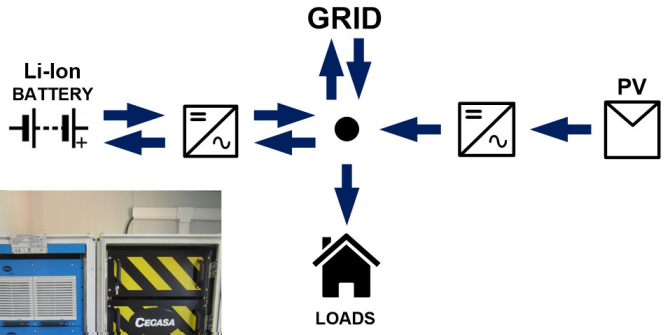

Lithium Ion Battery:

- 5kW nominal power
- 31.8kWh capacity
- 302.4 V Vmax / 194.4 V Vmin
- 5C (200A) max discharge
- 3C (120A) max charge

Battery Inverter: 5kW nominal power

PV installation: 3.224 kWp (a-Si)

PV inverter: 5kW nominal power

Self Consumption Optimization Strategy

Objective:
The main objective of this strategy is to maximize the consumption of locally produced PV power, hence minimizing the injection of power into the electrical grid.

Implementation:

$$P_{setBat} = P_{pv} - P_{load}$$

$$P_{grid} = P_{setBat} - P_{bat}$$

Due to battery operational limits (Voltage and SOC), a control to avoid overdischarge/charge was implemented.

P_{setBat}	AC Power command to battery inverters
P_{pv}	PV AC power
P_{load}	Loads AC power consumption
P_{grid}	AC Power exchange with the grid
P_{bat}	Measured battery inverters AC power

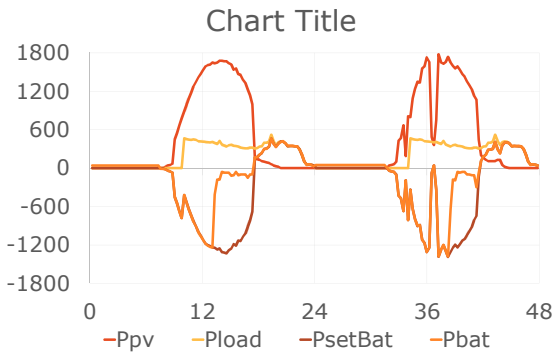

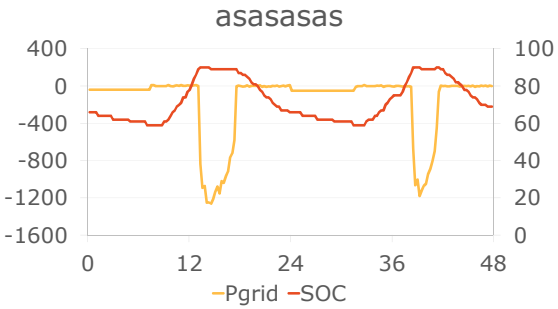

GOVERNO DE PORTUGAL
QUADRO DE REFERÊNCIA ESTRATÉGICO NACIONAL
ST Renewable Energies Chair
UNIVERSIDADE DE ÉVORA
PV CROPS
SEVENTH FRAMEWORK PROGRAMME
POPH QUALIFICAR É CRESCER.
UNIÃO EUROPEIA Fundo Social Europeu

GOOD AND BAD PRACTICES IN PV PLANTS

POLITÉCNICA
Instituto de Energía Solar

F. Martínez-Moreno (francisco.martinez@ies-def.upm.es), F. Helleputte (fhellepute@sunswitch.be), N. Tyutyundzhiev (pv-jet@phys.bas.bg), D. Rabal (daniel.rabal.echeverria@acciona.es), M. Conlon (michael.conlon@dit.ie), D. Oteiza (David.Oteiza@ingeteam.com), T. Fartaria (tomasfartaria@uevora.es)

5BV.4.15

1. INTRODUCTION

- Grid-connected PV sector is maturing and spreading all around the world.
  - More than 100 GW of BIPV and large PV plants have been installed only in 10 years (80 GW last 3 years).
  - PV solar energy is the 3rd most significant renewable energy source (behind hydro and wind energy in terms of capacity).
  - PV solar energy can compete in cost terms with traditional energy sources even without additional subsidies (South Europe).
- PVCROPS project has compiled a manual with a collection of good and bad practices detected in PV plants
  - New PV installation will be more and more competitive: more reliable, efficient and cost-effective if errors and mistakes already done are avoided.

2. GOOD AND BAD PRACTICES: THE MANUAL

- Objective: to represent a useful reference for when a new installation is being designed and built.
- 129 pages and 229 pictures with an explanatory text.
  - Pictures related to good practices: show how the installation has to be done.
  - Pictures related to bad practices: show examples of what has to be avoided.
  - Pictures are classified in 7 categories:
    - Civil works
    - Supporting structures
    - Connection boxes
    - PV array
    - Inverter
    - Monitoring
    - Others

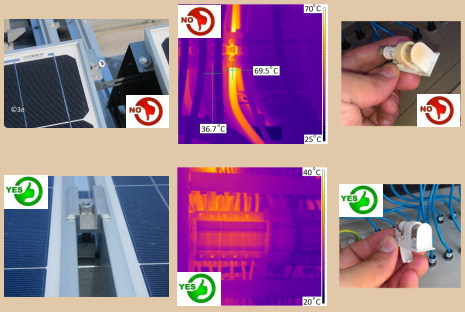

3. MANUAL DOWNLOAD

- "Good and Bad Practices: Manual to improve the quality and reduce the cost of PV systems" is free available
  - Visit www.pvcrops.eu
  - Different languages (soon): english, spanish, bulgarian, portuguese, french, dutch and arabian.

4. FUTURE OF THE MANUAL

- The manual will be periodically revised, improved and updated.
- All people is invited to collaborate (new situations and pictures are welcome).

GOOD AND BAD PRACTICES IN PV PLANTS

F. Martínez-Moreno[1], F. Helleputte [2], N. Tyutyundzhiev [3], D. Rabal [4], M. Conlon[5], T. Fartaria[6], D. Oteiza[7]

[1] Instituto de Energía Solar – Universidad Politécnica de Madrid. Grupo de Sistemas Fotovoltaicos (IES-UPM). Campus Sur UPM. Ctra. Valencia km. 7. EUIT Telecomunicación. 28031 Madrid, Spain. francisco.martinez@ies-def.upm.es
[2] Sunswitch. Av. Jean Monnet 1. B-1348 Louvain-la-Neuve. Belgium. fhellepute@sunswitch.be
[3] Central Laboratory of Solar Energy & New Energy Resources. 1784 Sofia, 72 Tzarigradsko chaussee Blvd. Nuclear Centre 7th km. pv-jet@phys.bas.bg
[4] Acciona Energía, Spain. Avda. Ciudad de la Innovación 5. 31621 Sarriguren. Navarra. Spain. daniel.rabal.echeverria@acciona.es
[5] DIT Hothouse. Dublin Institute of Technology, Ireland. Aungier Street, Dublin 2, Ireland. michael.conlon@dit.ie
[6] Cátedra BES – Energias Renováveis. Universidade de Évora. Casa Cordovil 2º Andar. Rua Augusto Eduardo Nunes 7. 7000-651 Évora. Portugal. tomasfartaria@uevora.pt
[7] Ingeteam Power Technology, Avda. Ciudad de la Innovación 13. 31621 Sarriguren, Navarra. Spain. David.Oteiza@ingeteam.com

ABSTRACT: The PVCROPS project (PhotoVoltaic Cost r€duction, Reliability, Operational performance, Prediction and Simulation), cofinanced by European Commission in the frame of Seventh Framework Programme, has compiled in the "Good and bad practices: Manual to improve the quality and reduce the cost of PV systems" a collection of good and bad practices in actual PV plants. All the situations it collects represent the state-of-the-art of existing PV installations all around Europe. They show how the different parts of an installation can be implemented properly or not. The aim of this manual is to represent a reference text which can help any PV actor (installers, electricians, maintenance operators, owners, etc.) not only to check and improve an already existing installation but will also, and mainly, avoid the previously known bad practices for the construction of a new PV installation. Thus, solving a priori the known errors, new PV installations will be more reliable, efficient and cost-effective and can recover the initial investment in a shorter time. The manual is going to be free available in the PVCROPS website in several languages.

Keywords: PV System, grid-connected, reliability, cost reduction, education and training

1 INTRODUCTION

Grid-connected photovoltaic (PV) solar energy is a technology which has come to play a significant role in the electricity generation and supply systems of many countries. Over a period of only 10 years, approximately 100 GW of PV capacity has been developed and constructed with close to 80 GW of that total having been built in the past 3 years. This represents an annual grown of close to 40%. For this reason, PV installations are the third most significant renewable energy source, behind hydro and wind energy in terms of capacity. This exponential growth has been evident in Europe, where close to 70% of the worldwide grid-connected PV power is situated. In fact, some European countries are meeting more than 5% of their annual electricity demand with PV energy (Germany and Italy) [1]. This rapid development has been accompanied by a gradual decrease of PV device costs, and this has propitiated that, in the south of Europe, PV solar energy now can compete in cost terms with traditional energy sources (gas, coal, oil, nuclear, etc.), even without additional subsidies.

The PV sector is maturing and spreading rapidly elsewhere in the World. Evidence of this is that last year (2012) was the first year in which PV power installed in the rest of the word was almost at the same level as that installed in Europe [1]. In order to continue with this growth, and to make PV solar energy more and more competitive, it is necessary to consider the best practices for PV installations. This involves avoiding the mistakes which occurred in the earlier installations. Thus, solving a priori the known errors, new PV installations will be more reliable, efficient and cost-effective and can recover the initial investment in a shorter time.

So, the PVCROPS project (PhotoVoltaic Cost r€duction, Reliability, Operational performance, Prediction and Simulation) has compiled in the "Good and bad practices: Manual to improve the quality and reduce the cost of PV systems" [2] a collection of pictures that show the good and bad practices which have been detected in existing PV installations.

This manual is inspired in a previous text related to rural electrification that reports about good and bad practices in PV stand-alone installations [3].

2 GOOD AND BAD PRACTICES: MANUAL

2.1 Objectives.

The main objective of the manual is to represent a useful reference for when a new installation is being designed and built. The good practices will be examples of how to implement these projects to get each individual device operating properly and avoid premature degradation. The bad practices will be example of mistakes which have previously been made and should be avoided.

The fact that this manual shows bad practices should not be interpreted as indicating that they are common in existing installations. On the contrary, PV installations are generally well constructed and are operating effectively, with good practices predominating. The manual tries to show those defects that have been detected and which can cause a reduction in the lifetime of the installation or in the resulting energy production. Therefore, such practices lead to a decrease in overall performance if they are not resolved.

The examples shown in the manual are related to

both PV plants and building integrated photovoltaic systems (BIPV). Most of the situations and examples it presents come from PV plants, but there are good and bad practices common in both installations.

It is necessary to point out that all the measures recommended in the manual are worthless if after a PV installation is built, it is not properly maintained. Following the recommendations presented in the manual will not guarantee a good performance from a PV installation. PV installations must meet the national electrical industry regulations and should include preventive and corrective maintenance to detect and quickly solve faults and failures that can appear during normal operation. It is advisable to install a monitoring system, operated by qualified personnel, that provides alerts in the event of faults in the PV installation during operation. A periodic review of the status and condition of the wiring, plugs, modules, inverters, etc. is essential. Only in this way the installation will operate properly, ensuring that it reaches its full design lifetime, a high availability level with high energy production and, consequently, lower costs for PV solar energy.

2.2 Organization

The manual is composed by 129 pages, including 229 pictures, and is divided in 4 chapters.

Chapter 1 is a brief introduction reporting the evolution of PV installation grid connected all around the world and the objectives of the manual.

Chapter 2 reports about the organization of the manual and explains how the manual is written.

Chapter 3 shows the good and bad practices which have been detected in existing PV installations. It is divided into 7 sections, each dealing with separate aspects of grid-connected photovoltaic installations, both PV plant and BIPV. These sections describe both typical good practice in terms of PV installations and some of the mistakes which can occur. The presentation is in the form of visual material, both photographs and diagrams, and a short text which describes the good and bad practice where relevant.

As noted above, each category is related to one of the main components or sub-systems of a PV system and is identified by a letter which indicates the aspect to which the figures refer:

- "C" for the civil works needed to implement the PV installation;
- "S" for the supporting structures holding the PV modules, the connection boxes and the cables;
- "W" for the connection boxes that save the live cables, fuses, switches and others devices from outdoors;
- "G" for the photovoltaic array or generator that transforms solar energy into electricity;
- "I" for the inverters that converts the DC power from the PV array to AC power to be injected into the grid;
- "M" for the monitoring devices and routines that supervise the operation of the installation and reports about it;
- "O" for those other aspects not dealt with the other categories, mainly those related with the integration of the installation in the environment.

All of the photographs are from real installations in various parts of Europe and represent the common procedures which are used for the construction of PV installations. Avoiding bad practices and applying the examples of better practice will help to ensure that final PV installations will be free of premature degradation and frequent failure that will decrease the energy production of the system and, consequently, its profitability.

Fig. 1 shows the symbols used to report about a good practice (left) a bad practice (middle) and a situation that is neither a good or a bad practice but could be improved (right). These symbols highlight quickly and clearly the nature of the situation being presented.

Figure 1: Symbols used to report about good practices (left), bad practices (middle) or a situation that could be improved (right).

Finally, chapter 4 gives some links to web pages and forums in which information about PV installations can be found: news, research articles, general reports, analysis of PV technology, etc.

2.3 Example

Fig. 2 and Fig. 3 are examples taken from the manual. They show a bad and a good practice, respectively, and come from the section related to PV arrays, reporting about modules placement and shading.

Figure 2: Grid-connected PV installation with a supporting structure that cast a shadow over the panels behind it.

Figure 3: Grid-connected PV installation without shading between consecutive rows.

Fig. 2 shows a structure that cast a shadow over the panels behind it. Fig. 3 shows an installation without shading between consecutive rows. The explanatory text joined to the pictures in the manual helps to understand the situation that is shown in the pictures: the distance between PV modules must be large enough to avoid shading between rows even for winter time at noon (the critical time for shading in static installations as the sun is lower in the sky). Otherwise, the performance can be reduced.

2.4 Download and languages

The manual is going to be free available in the PVCROPS website (www.pvcrops.eu) and can be downloaded soon in several languages: English, Spanish, Portuguese, Bulgarian, French, Dutch, and Arabic. Fig. 4 shows the cover of the English version of the manual.

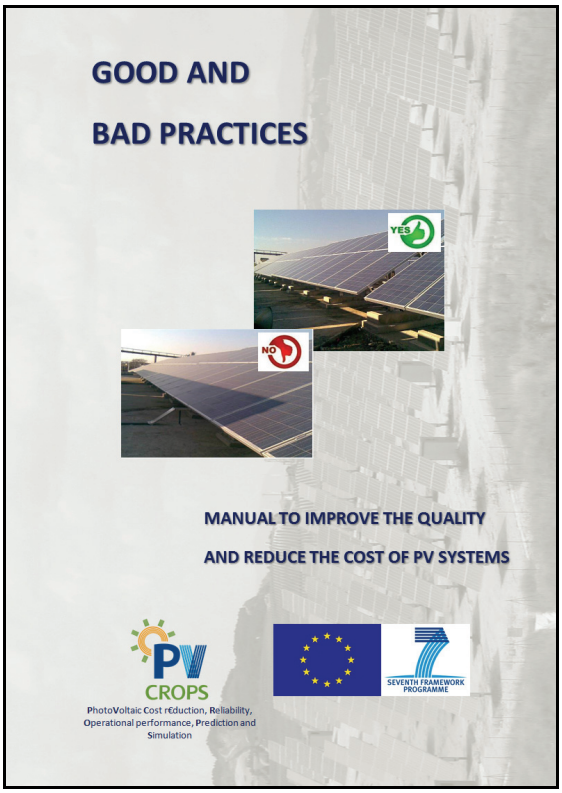

Figure 4: Cover of the "Good and bad practices: Manual to improve the quality and reduce the cost of PV systems".

3 FUTURE OF THE MANUAL

This manual is conceived to be a reference text not only in its origin, but also in the future. It pretends to be a "live" reference. The text and pictures here presented are the first version of a manual that will be periodically revised, improved and updated. So, this manual has been submitted to PV forums of different countries [4], [5], [6], [7] and translated to different languages to get the widest diffusion. All the people is invited to participate in these forums, reporting about those situations not collected here and sending the pictures that reflect the good or bad practices.

4 SUMMARY

This paper reports about the "Good and bad practices: Manual to improve the quality and reduce the cost of PV systems". This manual is composed by 129 pages, including 229 pictures that show the good and bad practices which have been detected in existing grid-connected PV installations. These practices are related with civil works, supporting structures, connection boxes, PV arrays, inverters, monitoring and others different aspects of an installation. The main objective of the manual is to represent a useful reference for when a new installation is being designed and built in order to avoid those defects previously done which can cause a reduction in the lifetime of the installation, in the resulting energy production or in the overall performance if they are not resolved.

5 ACKNOWLEDMENTS

The "Good and bad practices: Manual to improve the quality and reduce the cost of PV systems" has been written in the context of the PVCROPS project (PhotoVoltaic Cost r€duction, Reliability, Operational performance, Prediction and Simulation), that is cofinanced by European Commission in the frame of Seventh Framework Programme.

6 REFERENCES

[1] Global market outlook for photovoltaics 2013-2017. May 2013. European Photovoltaic Industry Association (EPIA, available in www.epia.org/news/publications/).
[2] Good and bad practices: Manual to improve the quality and reduce the cost of PV systems. PVCROPS Project (available in www.pvcrops.eu).
[3] Photovoltaic rural electrification: a fieldwork picture book. E. Lorenzo, R. Zilles, E. Caamaño. Promotora General de Estudios, S.A. Progensa (2001).
[4] http://solarweb.net
[5] http://forum-photovoltaique.fr
[6] http://apere.org/forum
[7] http://solar.st.bg/forum/index.php

UNIVERSIDADE DE ÉVORA
INSTITUTO DE INVESTIGAÇÃO
E FORMAÇÃO AVANÇADA

Contactos:
Universidade de Évora
Instituto de Investigação e Formação Avançada — IIFA
Palácio do Vimioso | Largo Marquês de Marialva, Apart. 94
7002 - 554 Évora | Portugal
Tel: (+351) 266 706 581
Fax: (+351) 266 744 677
email: iifa@uevora.pt